

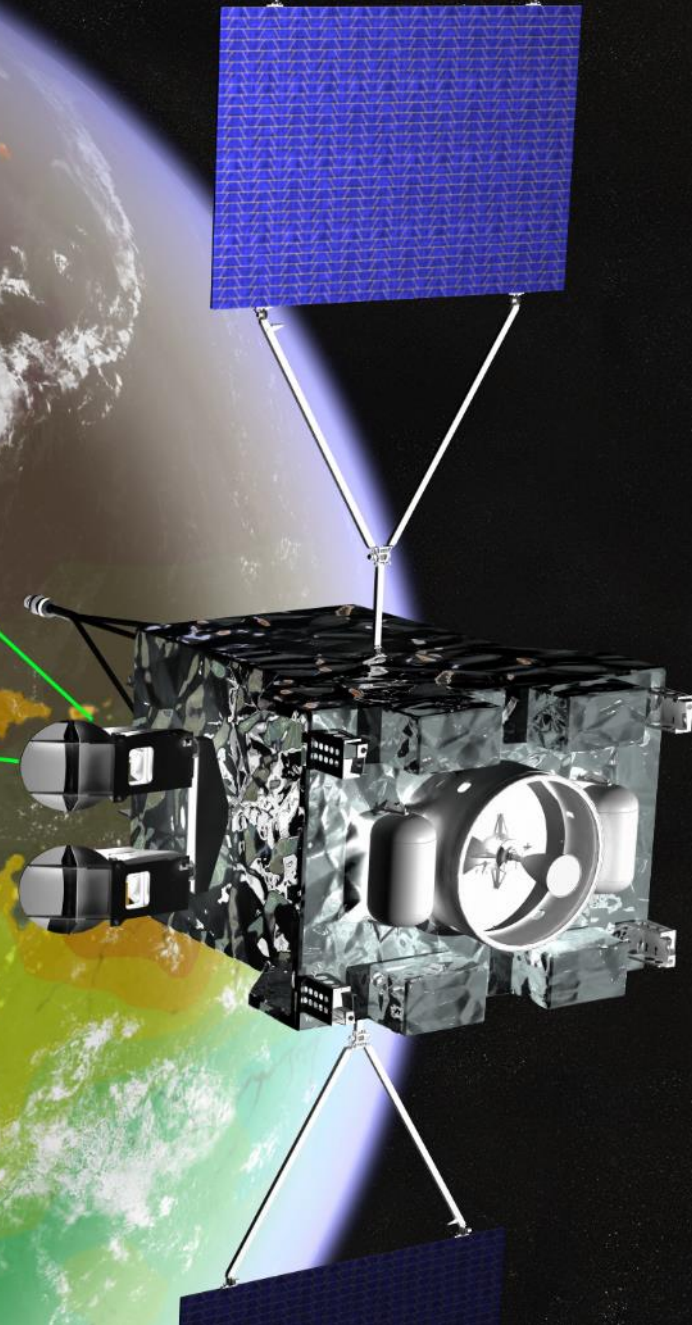


Pre-Launch and On Orbit Calibration of the GeoCarb Instrument: Lessons Learned from OCO and OCO-2

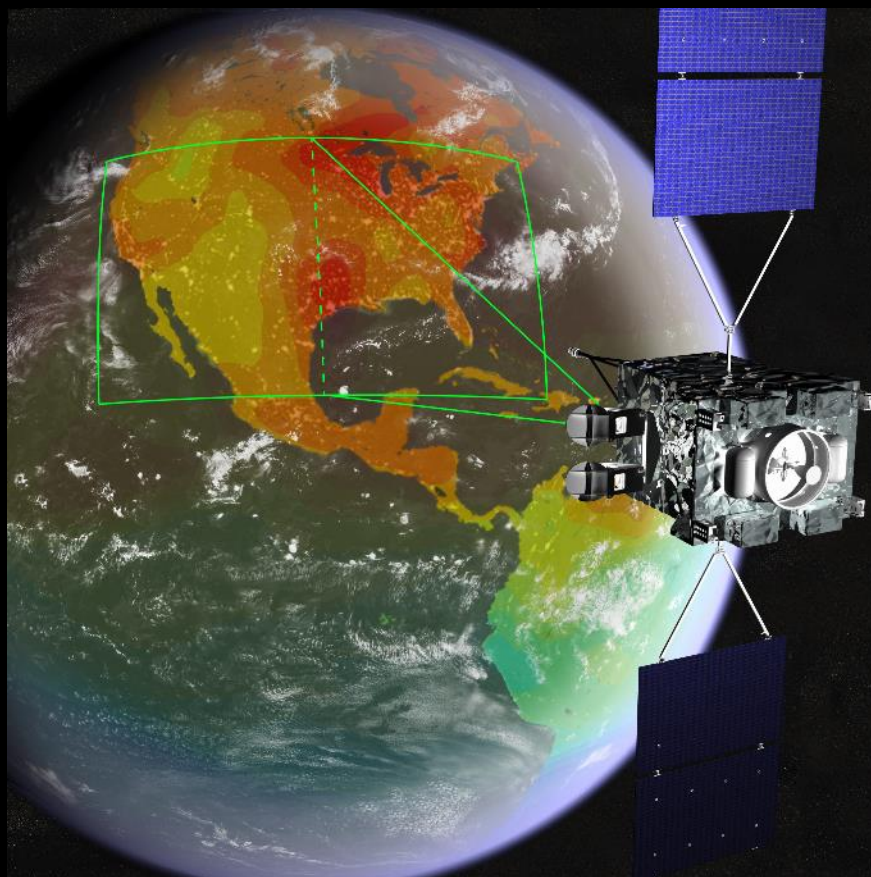
David Crisp
Jet Propulsion Laboratory,
California Institute of Technology

GeoCarb

The Geostationary Carbon Observatory

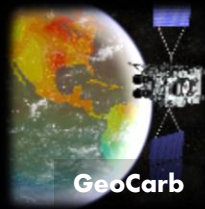


The GeoCarb Mission: Measuring Carbon Trace Gases and Vegetation Health from Space

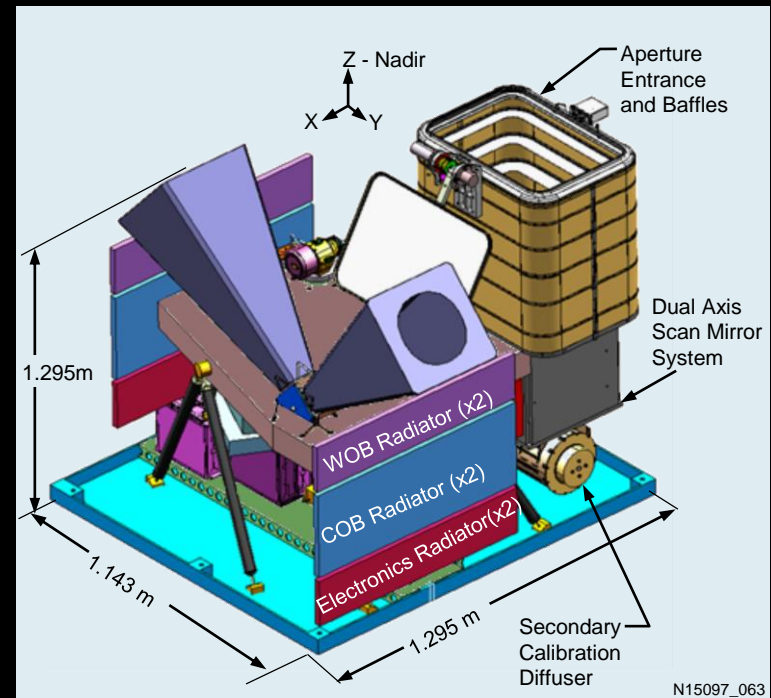
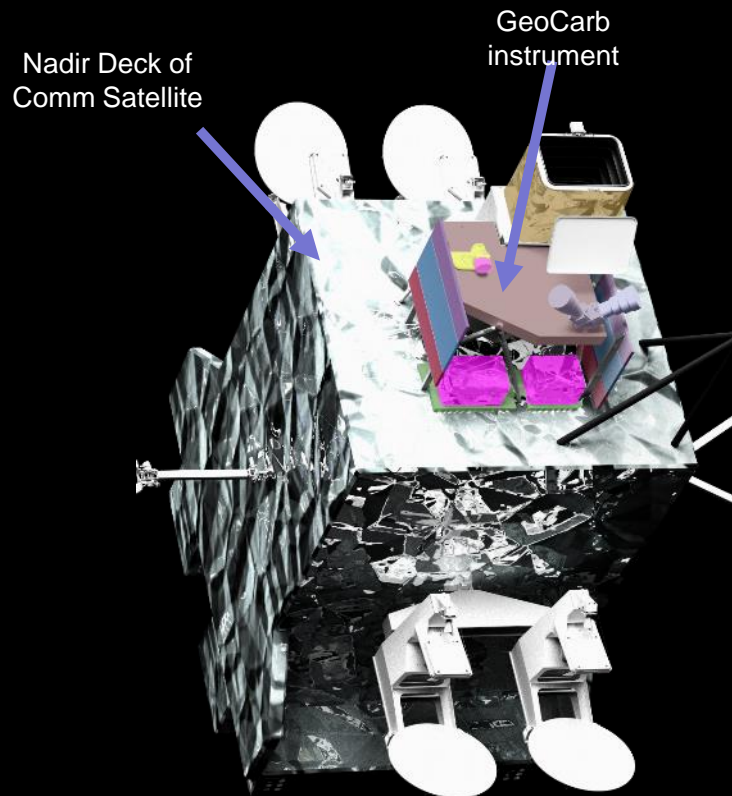


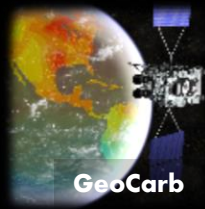
Principal Investigator Berrien Moore, University of Oklahoma
Technology Development Lockheed Martin Advanced Technology Center
Host Spacecraft & Mission Ops SSE Government Solutions

Instrument	Single slit, 4-Channel IR Scanning Littrow Spectrometer
Bands	0.76 μ m, 1.61 μ m, 2.06 μ m and 2.32 μ m
Gases	O ₂ , CO ₂ , CO, CH ₄ & Solar Induced Fluorescence
Mass	138 kg (CBE)
Dimensions	1.3 m x 1.14 m x 1.3 m
Power	128W (CBE)
Data Rate	10 Mbps
Daily Soundings	~10,000,000 soundings per day CONUS > once per day

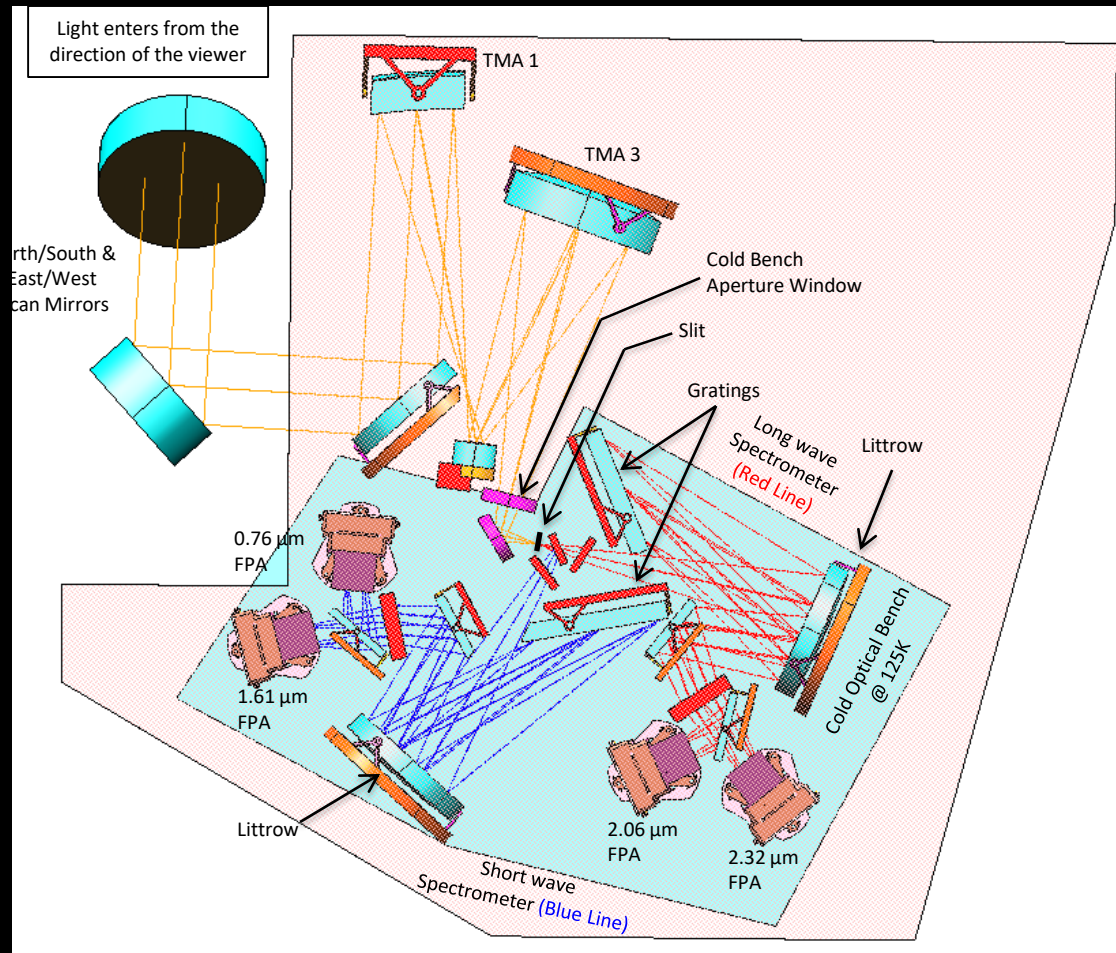
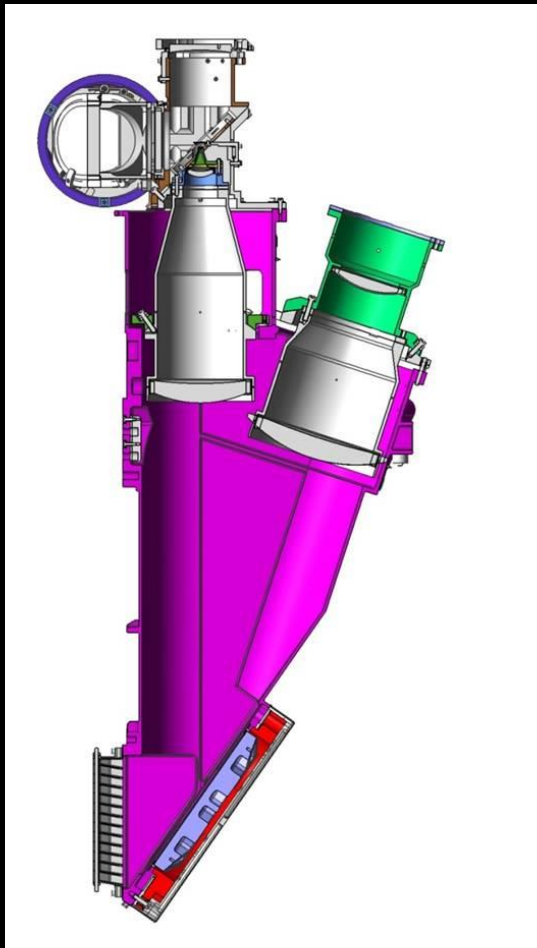


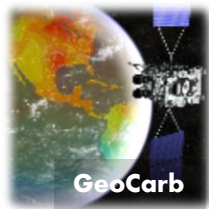
GeoCarb Instrument





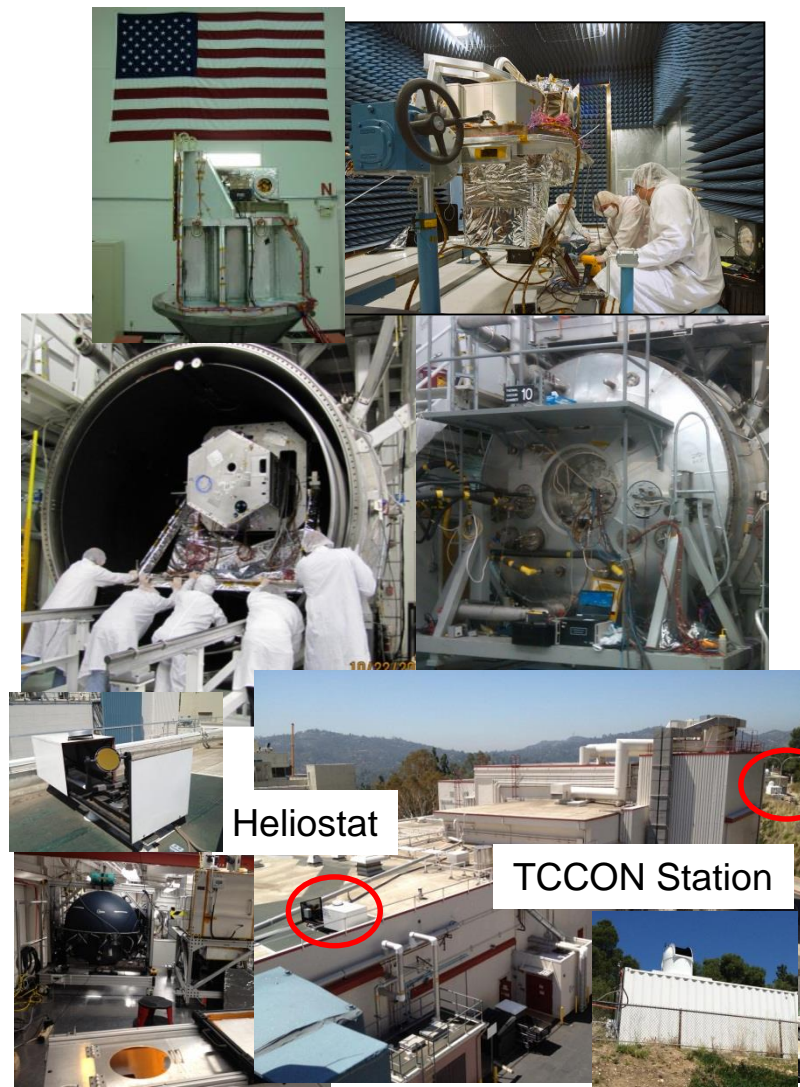
Pre-Launch and On Orbit Calibration of the GeoCarb Instrument: Lessons Learned from OCO and OCO-2

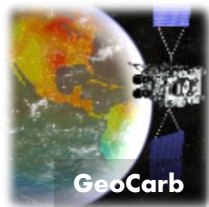




Pre-Flight Instrument Characterization and Calibration

- Pre-flight testing quantifies key Instrument performance and knowledge parameters
 - **Geometric**
 - Field of view, Bore-sight alignment
 - **Radiometric**
 - Zero-level offset (bias)
 - Gain, Gain non-linearity
 - **Spectroscopic**
 - Spectral range, resolution, sampling
 - Instrument Line Shape (ILS)
 - **Polarization**
 - **Instrument stability**

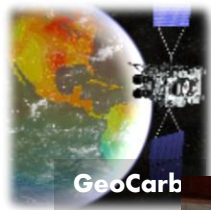




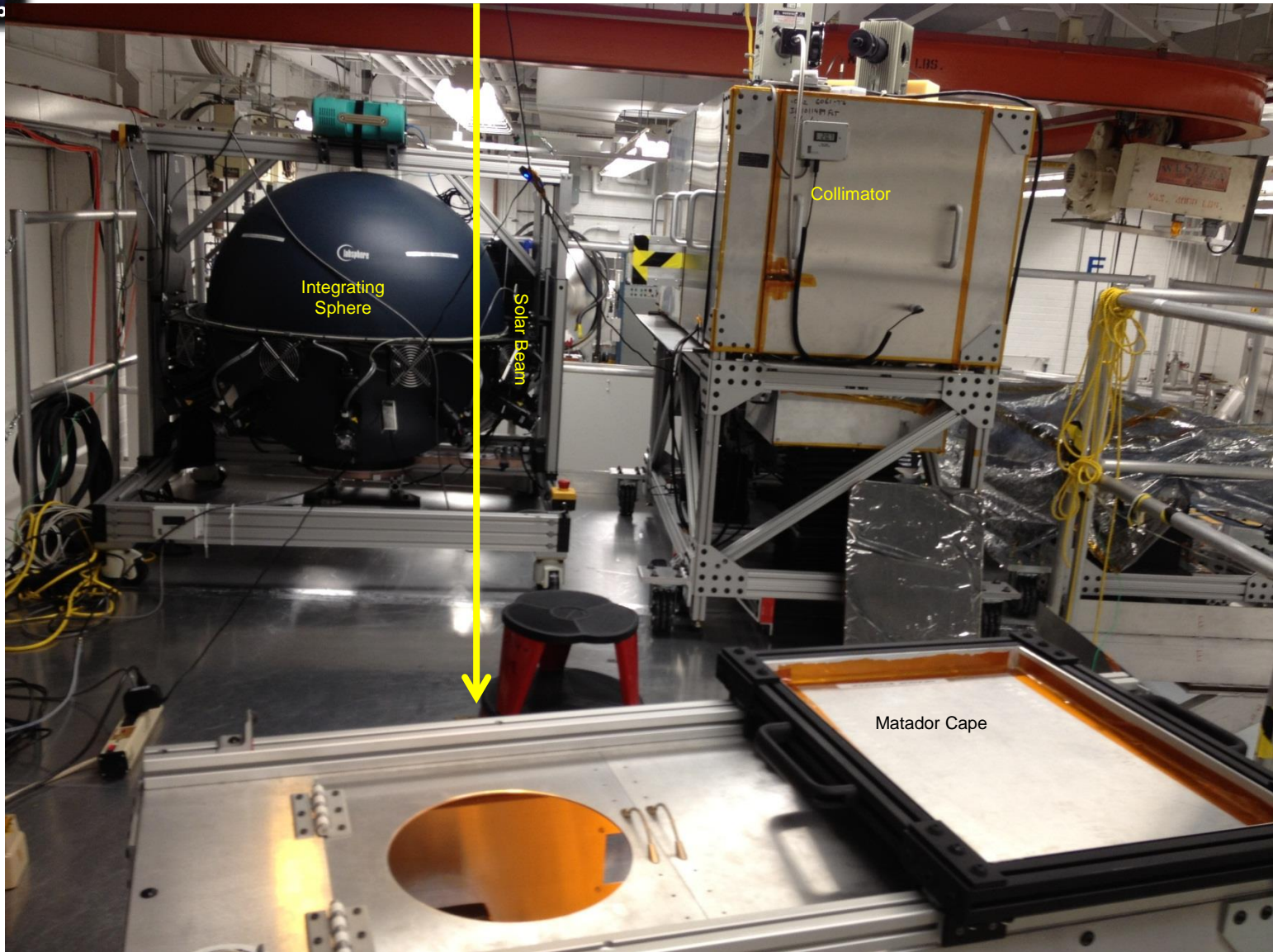
Optical Ground Support Equipment

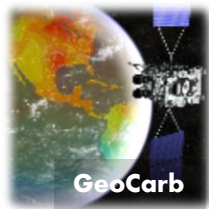
This test employed four types of optical ground support equipment

- **Collimator:** spatially-defined continuum and laser light sources to
 - Establish the spectrometer focus
 - Define the instrument field of view (including slit alignment, spatial stray light)
 - Define the spectrometer instrument line shape and spectral scattered light
 - Determine the angle of polarization
- **Integrating Sphere:** spatially uniform continuum light sources to
 - Characterize and calibrate radiometric performance (minimum and maximum measureable signal, radiometric gain and its linearity, signal to noise ratio)
 - Provide a baseline for the pixel-to-pixel variability in gain
- **Step-scan FTS:** for assessing spectral stray light rejection
- **Heliostat:** acquire atmospheric spectra using direct sunlight
 - Validate the instrument line shape and dispersion
 - Test the instrument linearity and transient response over a range of illumination levels
 - Provide an end-to-end test of instrument calibration & retrieval algorithm performance, through comparisons with TCCON XCO₂ retrievals



Calibration Deck

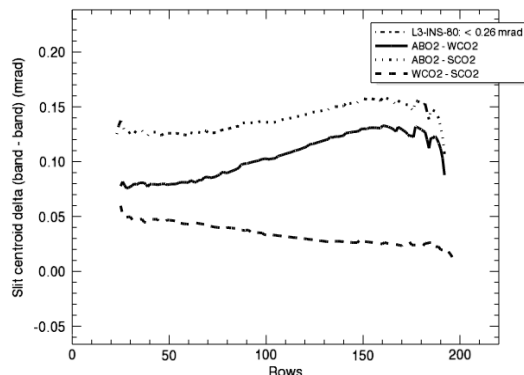




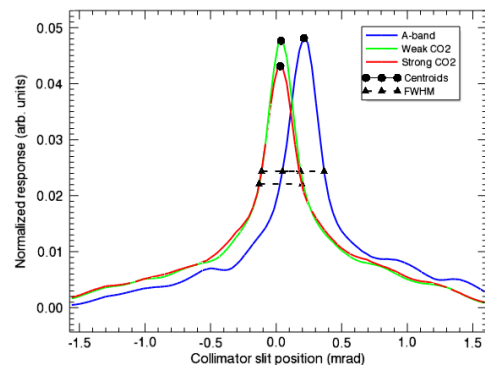
Geometric: Slit Alignment

Requirement	Value	Measured	Notes
Slit Width	< 2 mrad	~ 0.5 mrad (typical) 0.7 mrad (worst case)	~3x Margin
Slit Misalignment	< 0.26 mrad	~ 0.1 mrad (typical) 0.15 mrad (worst case)	~70% Margin

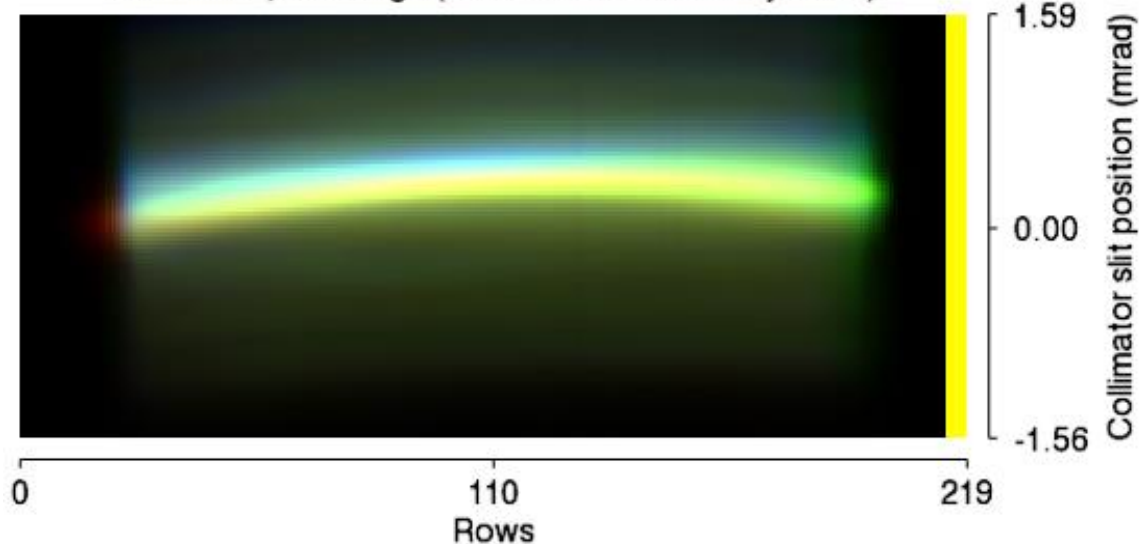
Test: 0260, Relative slit alignment



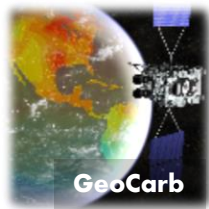
Test: 0253, Color slice (area normalized): row=100



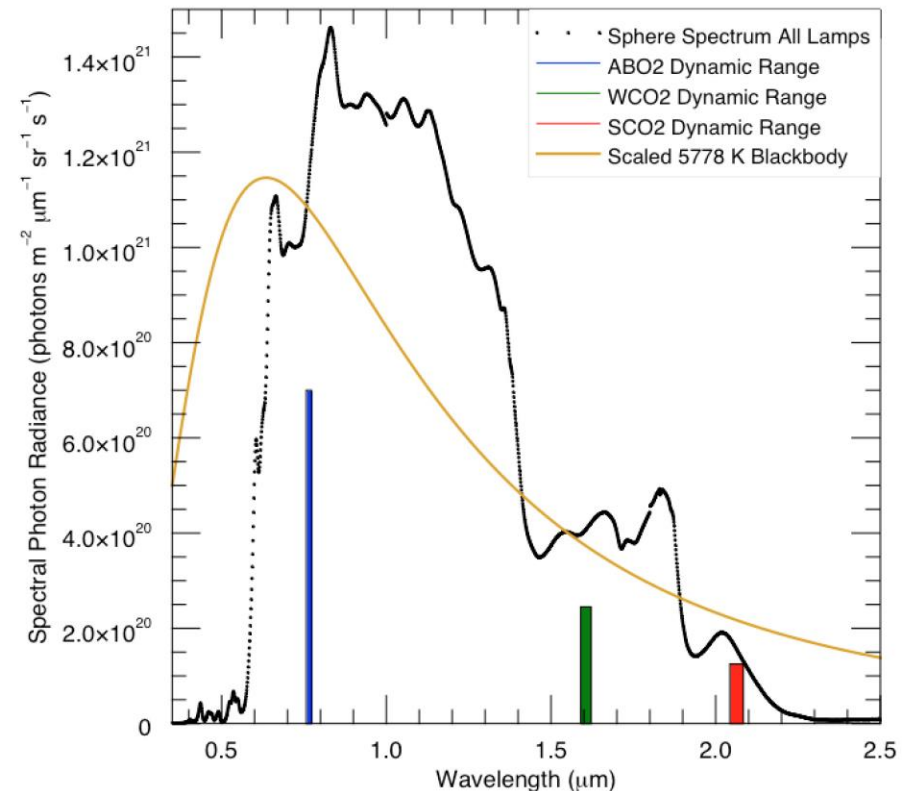
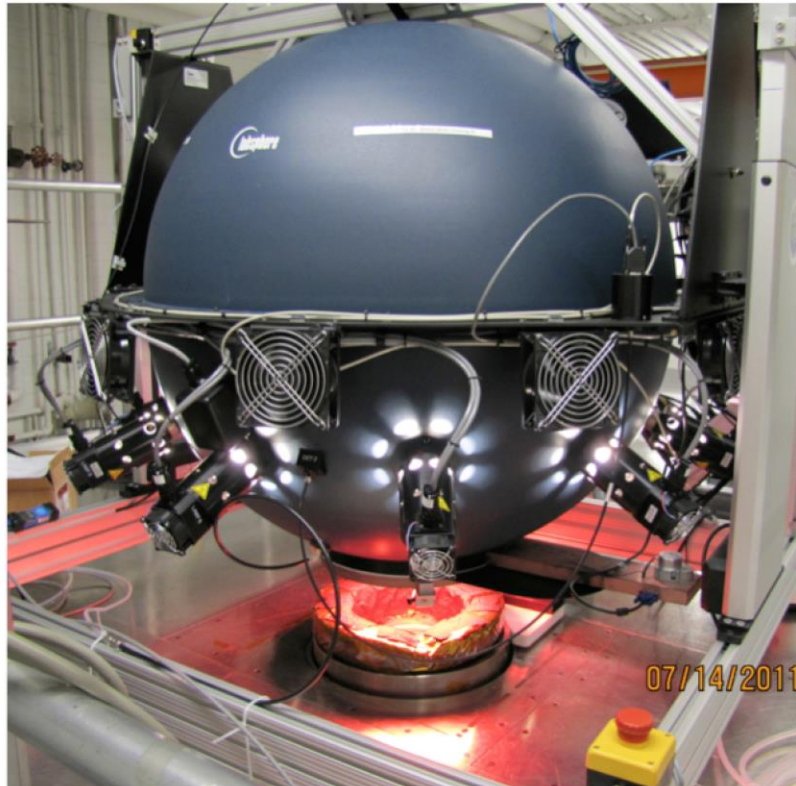
Test: 0260, Slit image (rows not measured="yellow")



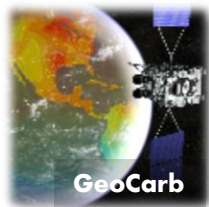
Impacts of slit misalignment and scene non-uniformity mitigated by defocusing the entrance telescope.



Radiometric Calibration with the Integrating Sphere

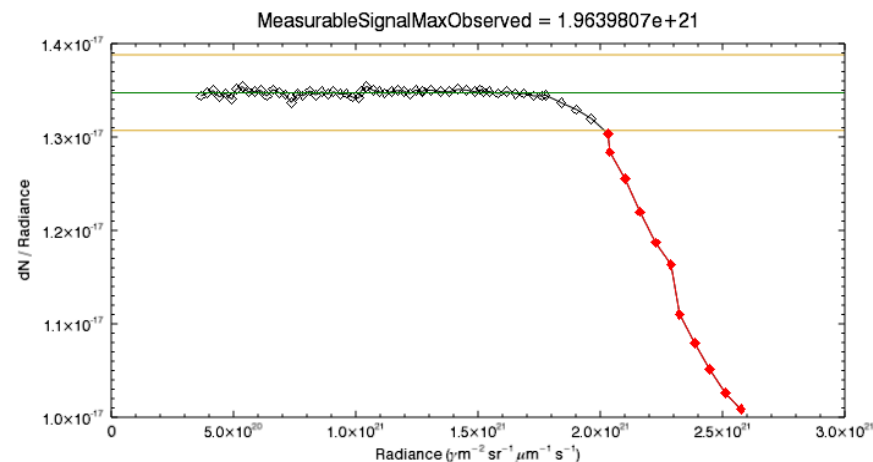
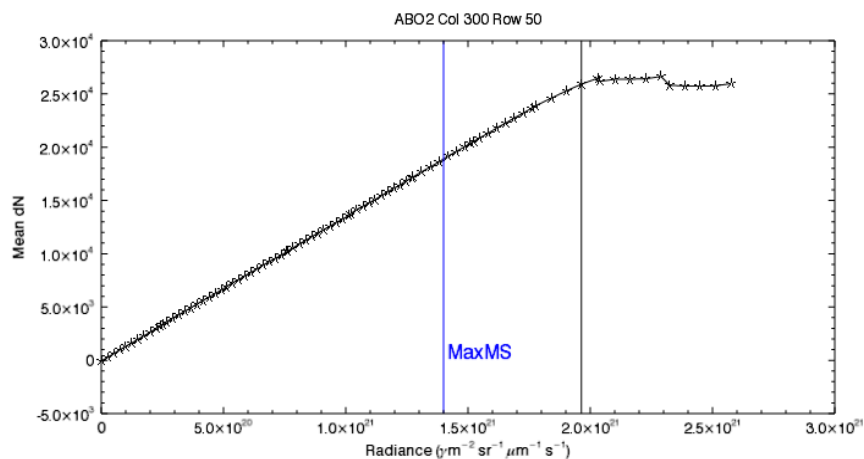


An integrating sphere with 10 lamps (one of which had a variable aperture) was the primary tool used for calibrating the radiometric performance of the instrument. The performance of the sphere (installed above the TV chamber in the TV test configuration) was calibrated in collaboration with NIST.

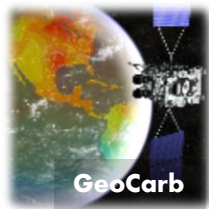


Radiometric: Dynamic Range

Requirement	Value	Measured	Notes
Max Measureable Signal – A-band	$\geq 1.4 \times 10^{21} *$	$\sim 1.8 \times 10^{21} *$	• ~30% Margin
Max Measureable Signal – Weak CO ₂	$\geq 4.9 \times 10^{20} *$	$> 8.7 \times 10^{21} *$	• Very large margins • Sphere isn't bright enough to saturate the detectors in CO ₂ channels
Max Measureable Signal – Strong CO ₂	$\geq 2.5 \times 10^{20} *$	$> 3.8 \times 10^{21} *$	

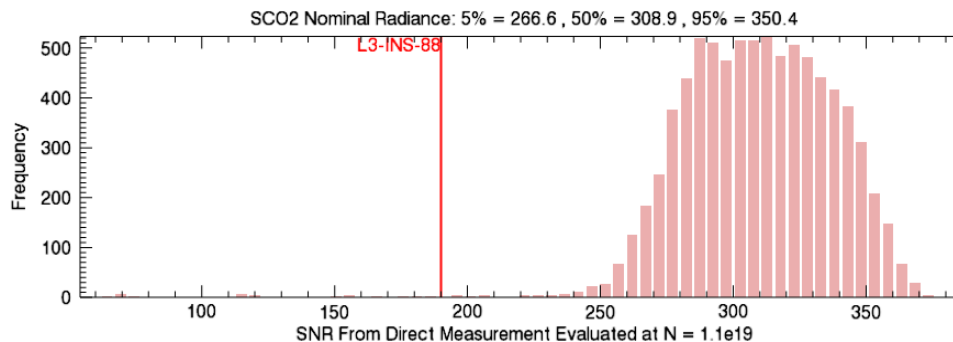
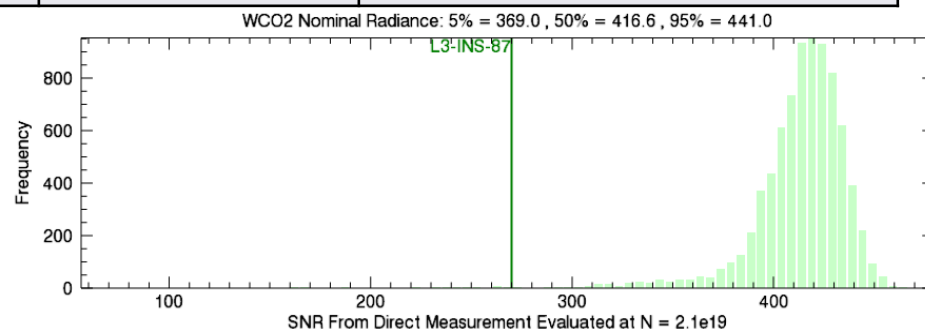
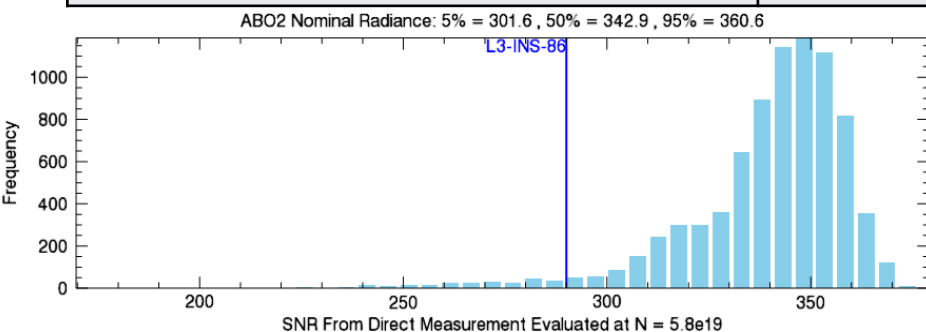


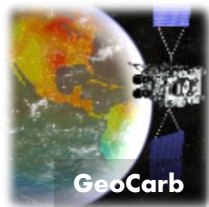
* OCO Radiance Units are: photons/m²/sr/μm/s



Radiometric: Signal-to-Noise Ratio at Nominal Signal

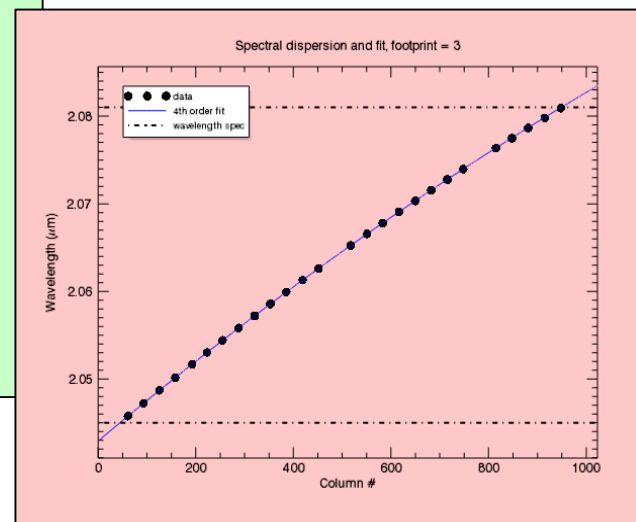
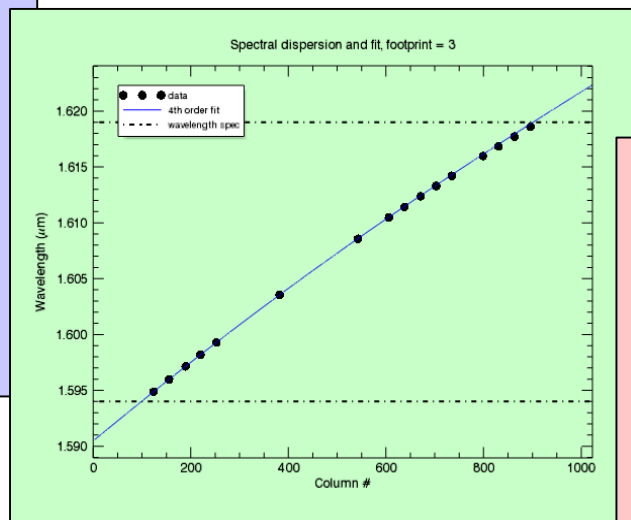
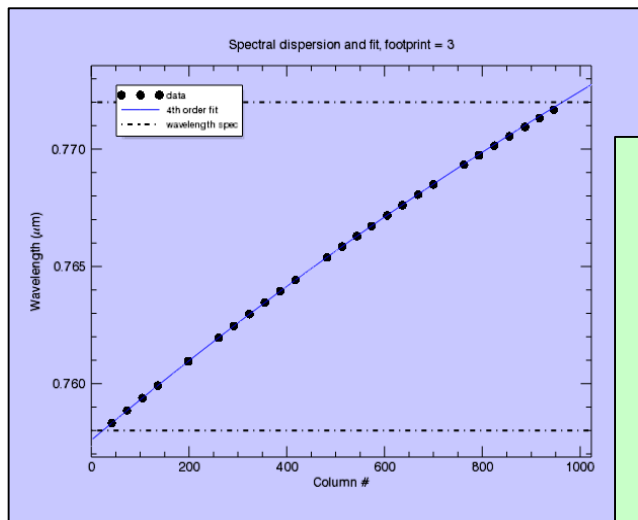
Requirement	Value	Measured	Notes
Signal-to-Noise Ratio – A-band	> 290	302 – 361	At 5.9×10^{19} photons/m ² /sr/μm/s
Signal-to-Noise Ratio – Weak CO ₂	> 270	369 - 441	At 2.1×10^{19} photons/m ² /sr/μm/s
Signal-to-Noise Ratio – Strong CO ₂	≥ 190	267 - 350	At 1.1×10^{19} photons/m ² /sr/μm/s

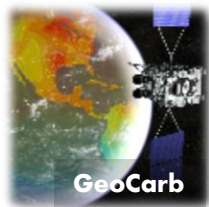




Spectroscopic: Spectral Range

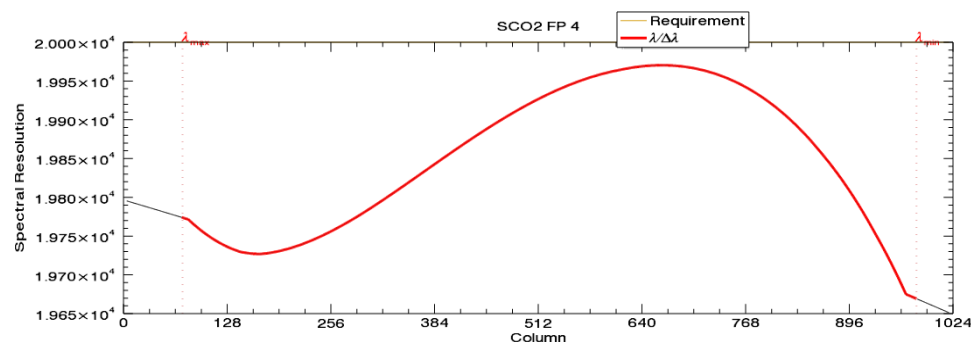
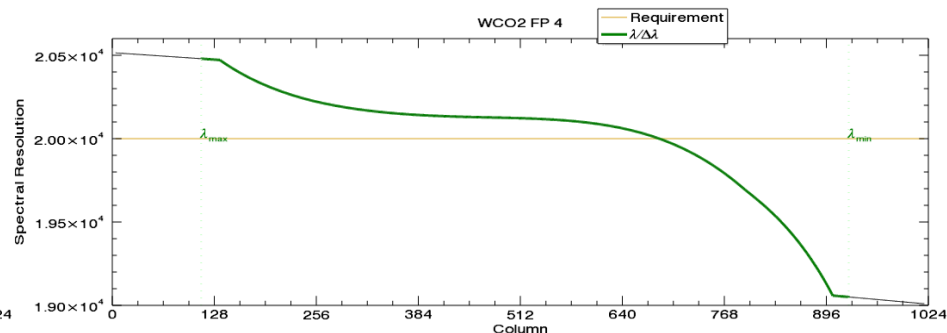
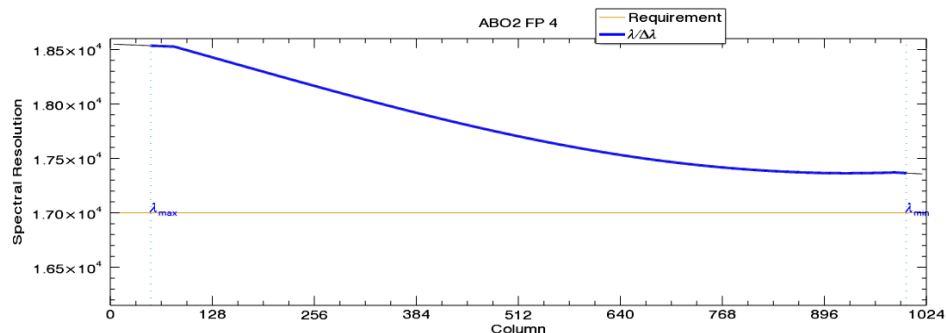
Requirement	Value	Measured	Notes
Spectral Range – A-band	758 to 772 nm	757.6 – 772.6 nm	Bands are well centered for OCO-2
Spectral Range – Weak CO ₂	1,594 – 1,619 nm	1,590.6 – 1,621.8 nm	
Spectral Range – Strong CO ₂	2,045 – 2,082 nm	2,043.1 – 2083.3 nm	

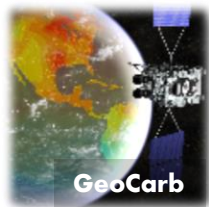




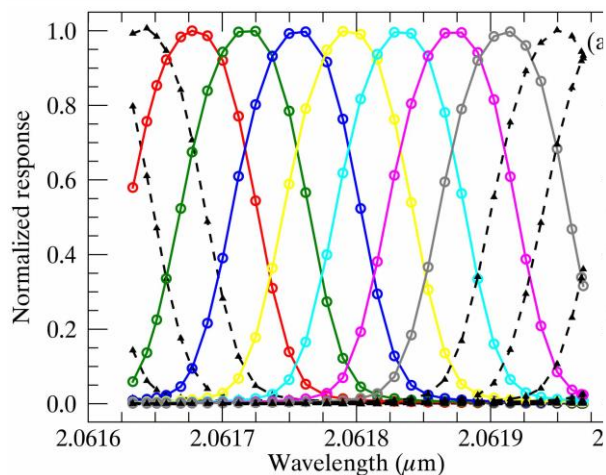
Spectroscopic: Spectral Resolution

Requirement	Value	Measured	Notes
Spectral Resolution – A-band	> 17,000	17,500 – 18,500	Resolving power is slightly low in CO ₂ channels. L2 Algorithm Team found no impact on OCO-2 Level 1 requirements
Spectral Resolution – Weak CO ₂	> 20,000	19,100 – 20,500	
Spectral Resolution – Strong CO ₂	> 20,000	19,700 – 19,900	

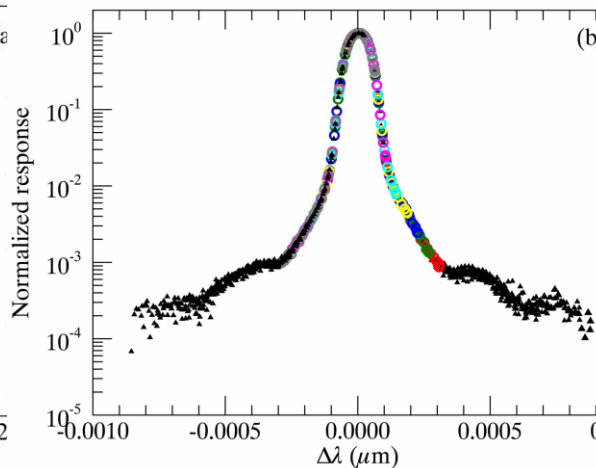




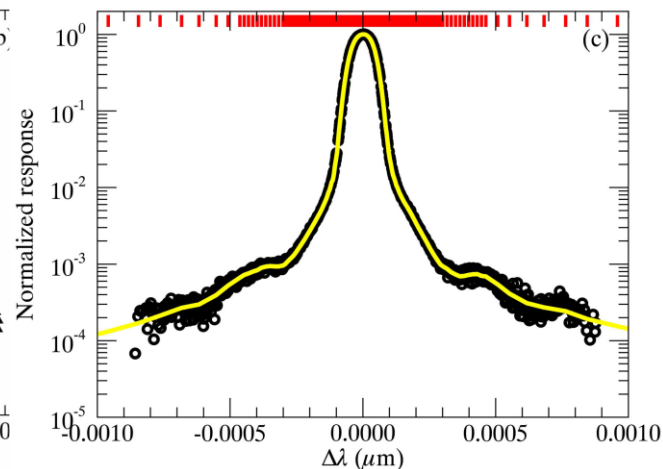
Characterizing the Instrument Line Shape (ILS) with Tunable Diode Lasers



Record Laser Diode Scans over 5-10 adjacent spectral samples at 40 to 50 wavelengths ranges throughout each channel.

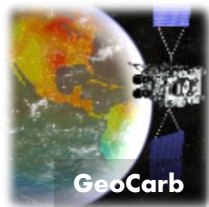


Combine measurements from all scans of each spectral sample within each scan range to create an over-sampled combined dataset



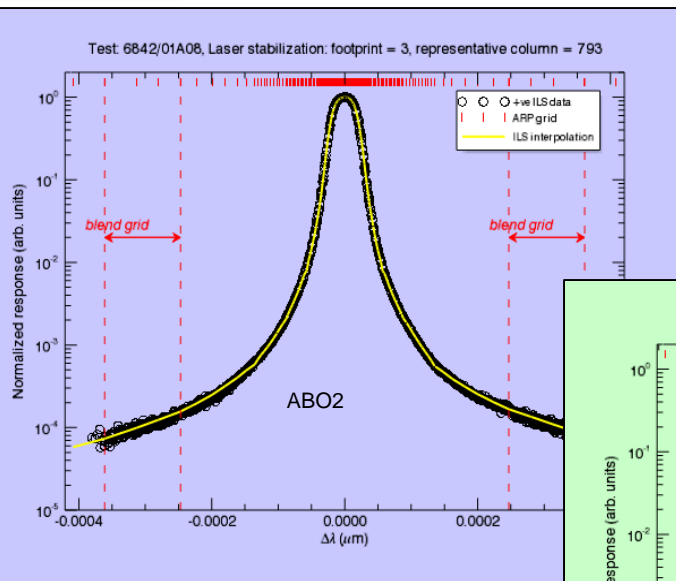
Produce a smooth fit to the combined data set for each sample.

Finally, the ILS was assumed to vary smoothly over each channel such that the mean ILS recorded for each 5-10 sample range can be attributed to the center wavelength of that range, and the ILS of intermediate samples can be linearly interpolated between these ranges. The ILS of each spectral sample is then described on a un-equally-spaced 200-point grid (see red dashes in figure above).

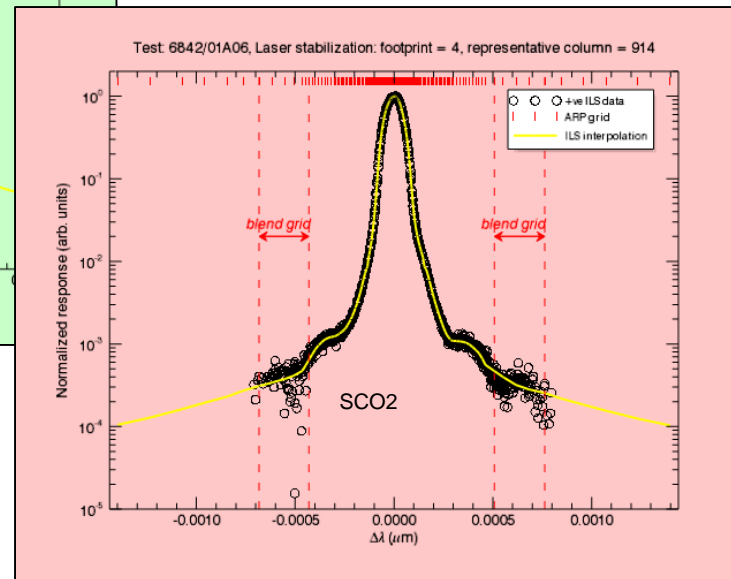
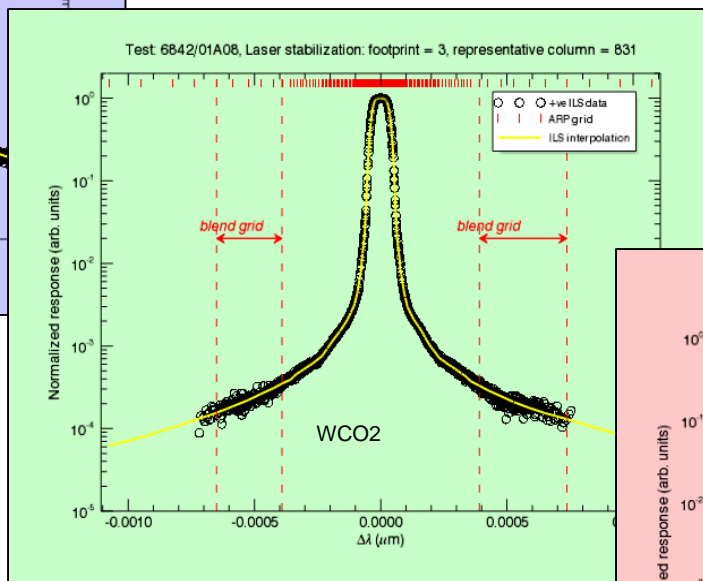


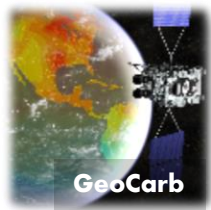
Spectroscopic; Instrument Line Shapes

- Examples of tunable diode lasers scans across each of the three spectral ranges.
- This method could characterize the ILS shape over a dynamic range of 1000 to 10000.

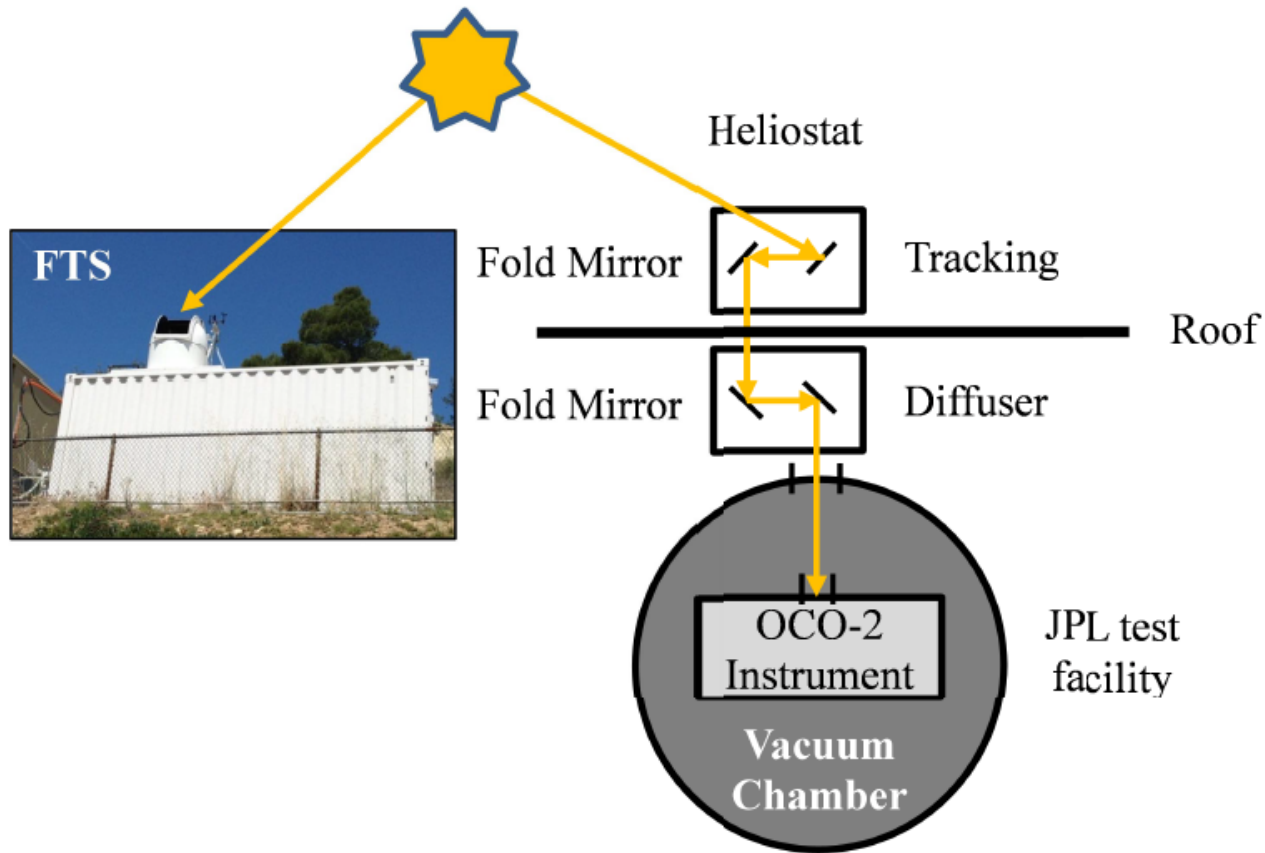


These results provided valuable information about the ILS shape, width (resolving power) and dispersion, but these results were not adequate to meet the OCO-2 requirements

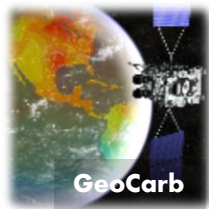




Verifying the ILS with Direct Solar Measurements



A heliostat on the roof of the building housing the thermos vacuum chamber allowed the acquisition of spectra of direct sunlight. Simultaneous observations from a nearby TCCON station served as a high resolution reference standard.

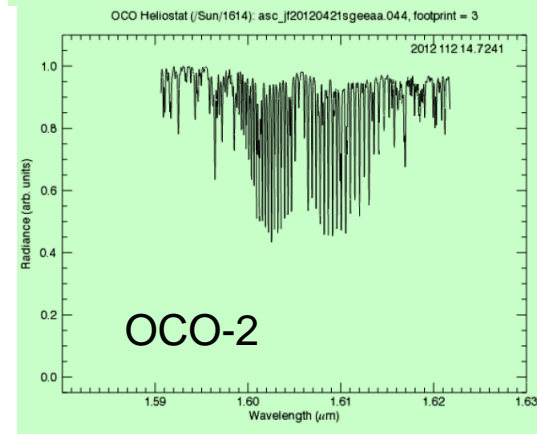
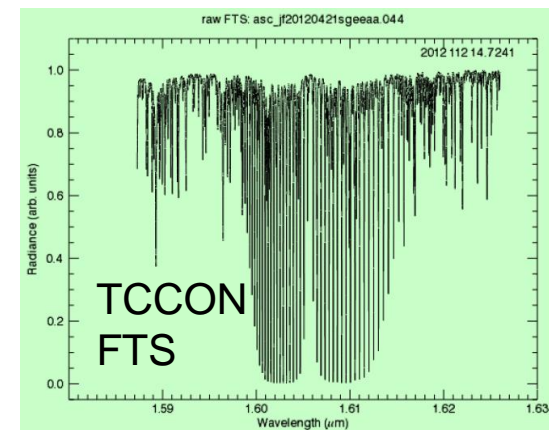


Pre-flight Heliostat/TCCON Observations Verify End-to-End Instrument Performance

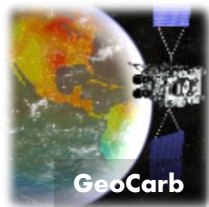
Observations of the sun with the flight instrument taken during TVAC tests provide an end-to-end verification of the instrument performance.



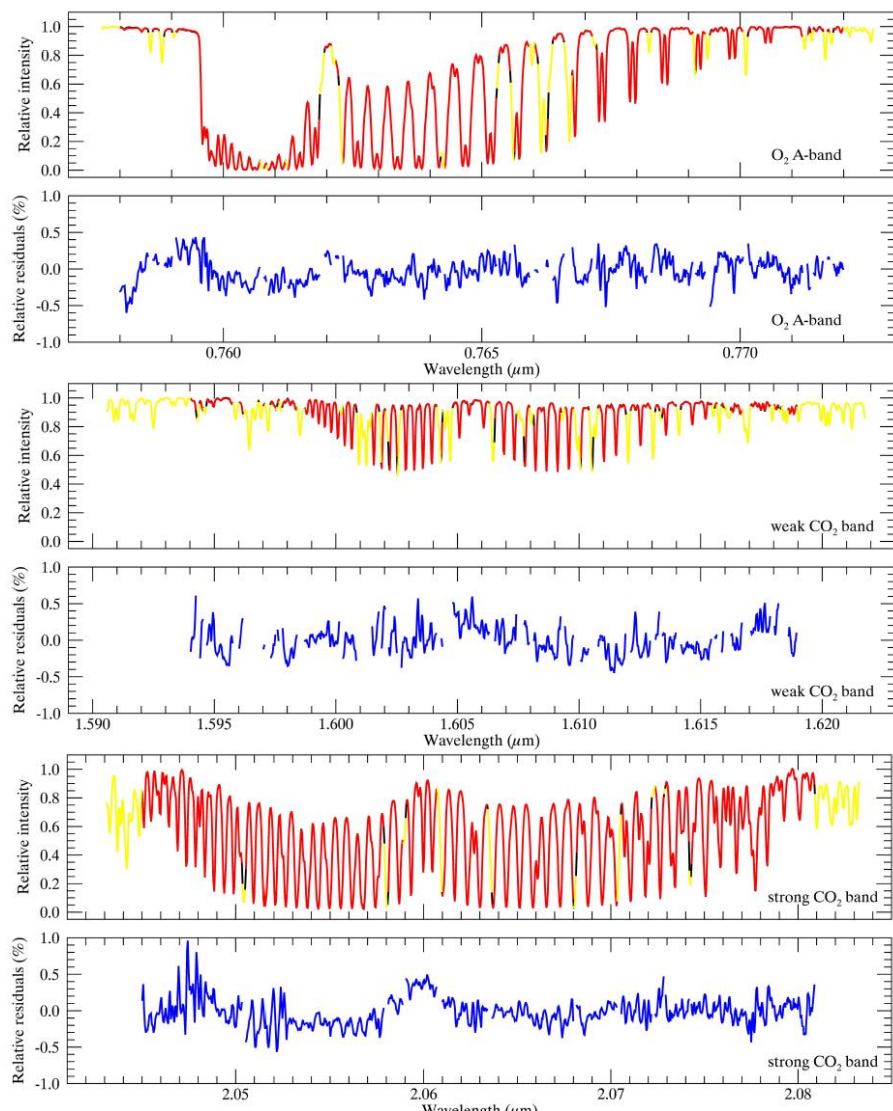
1.6 μm CO₂



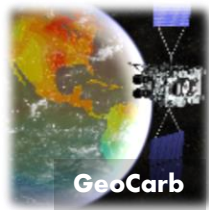
21 April 2012



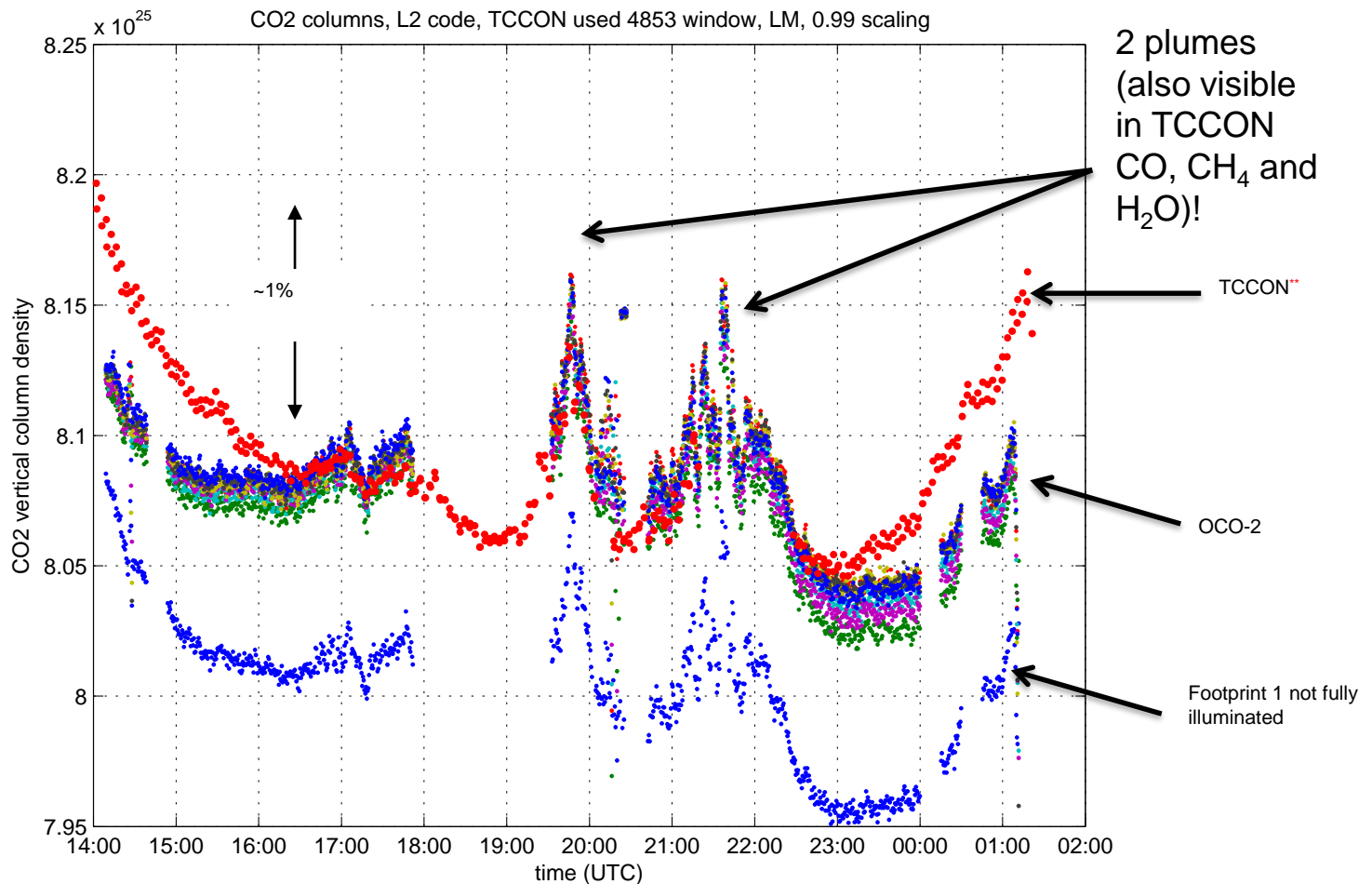
Example of OCO-2/TCCON Fits



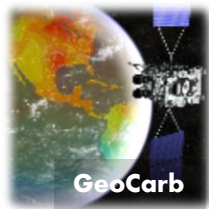
- TCCON spectra ($R \sim 200,000$) were convolved with the OCO-2 ILS fits derived from the laser diode measurements and compared to the spectra recorded by the OCO-2 instrument
- Strong solar lines had to be eliminated from these fits because the TCCON and OCO-2 sample the solar disk in differently
 - TCCON observes only the middle $\sim 10\%$ of the solar disk
 - OCO-2 samples the complete disk, including the solar limbs, and thus sees lines with more Doppler broadening.
- Typical residuals were $< 0.5\%$ after an optimization step (ILS width and dispersion adjusted)



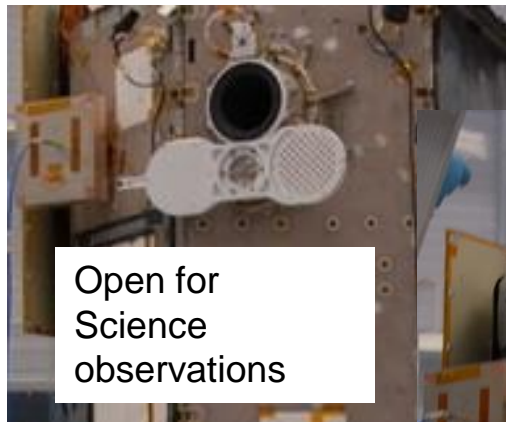
CO₂ Column Retrievals from the Strong CO₂ (SCO2) Channel at 2.06 μm



7 of the 8 footprints in the SCO2 channel produce CO₂ column estimates within $\pm 0.25\%$.
** TCCON does not use this channel to retrieve X_{CO_2} . This is a custom retrieval by D. Wunch.



Verifying Radiometric Calibration: The On-board Calibration System



Closed for lamp
calibration



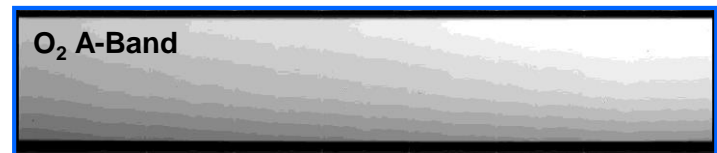
Reflective diffuser



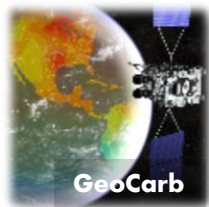
Telescope baffle assembly,
showing lamps for flat fields

The on-board calibration (OBC) system consists of a rotating calibration paddle that carries:

- an aperture cover, with a reflective diffuser illuminated by on-board lamps for monitoring pixel-to-pixel variations
- A transmission diffuser for making observations of the solar disk for monitoring radiometric calibration



Lamp “flat fields” from each channel.



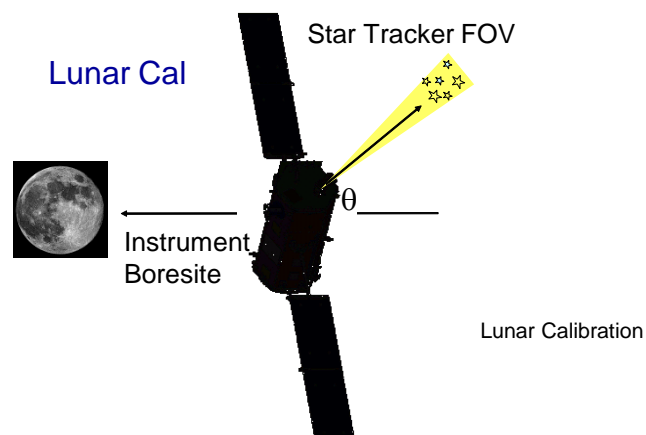
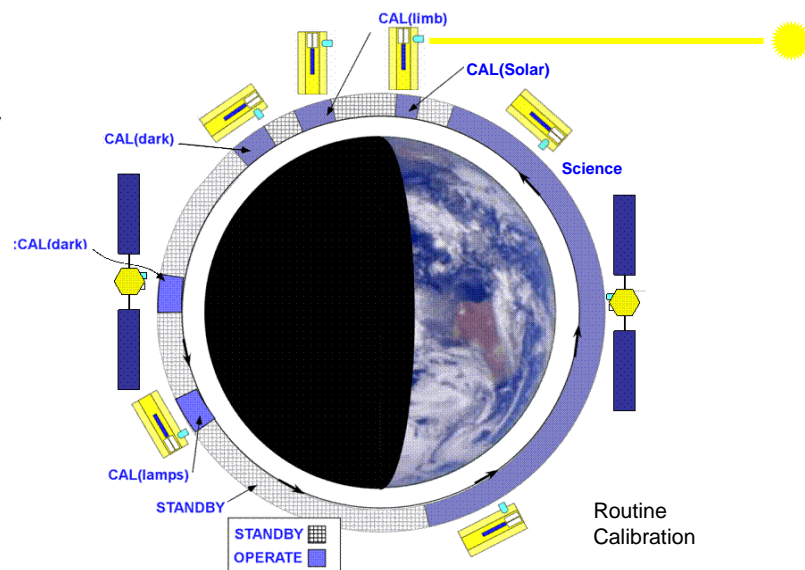
On-orbit Calibration Operations

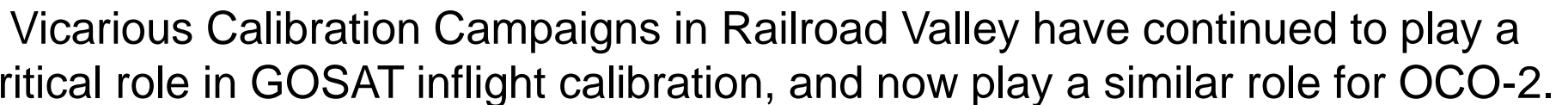
Routine Calibration (every orbit)

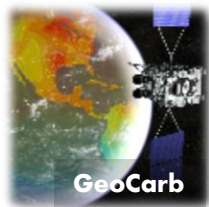
- OCO-2 will look at the sun through a solar diffuser
- Dark calibration with aperture door closed and lamps off

Special Calibration Activities

- Solar Doppler calibration
 - Observe sun through an entire daylight side of an orbit to calibrate ILS
 - once every six months)
- Lunar calibration required for absolute and relative pointing
 - Verifies alignment between instrument bore sight and the star tracker.
 - Used in radiance calibration
 - performed once every lunar month







Launch – And the show begins!



Credit: Bill Ingalls, NASA

Lift-off at 2:56 am
PDT, 02 July 2014

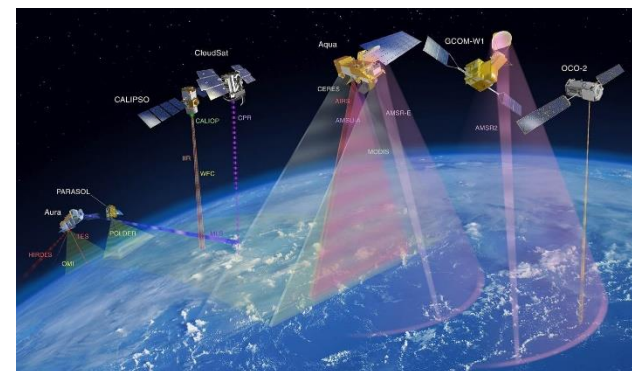


Credit: Jeff Sullivan

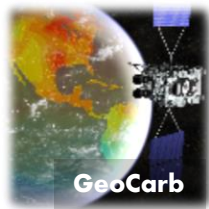


Credit: NASA

Separation!

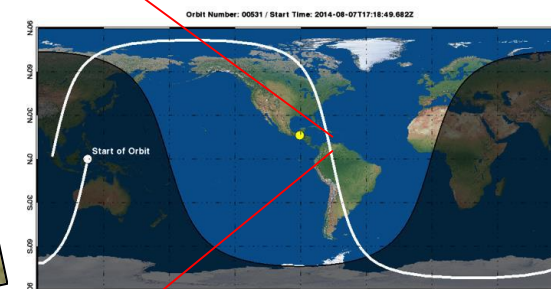
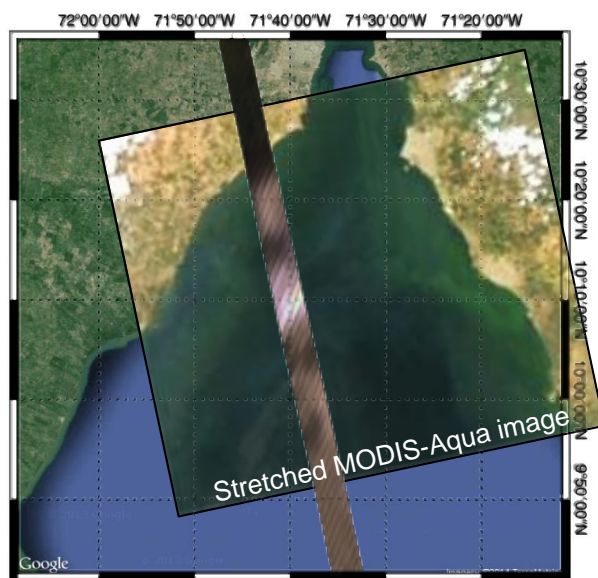


Joining the A-Train
3 August 2014

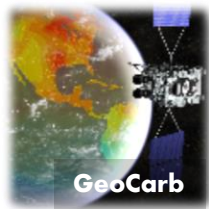


The Lake Maracaibo Incident, 7 Aug 2014

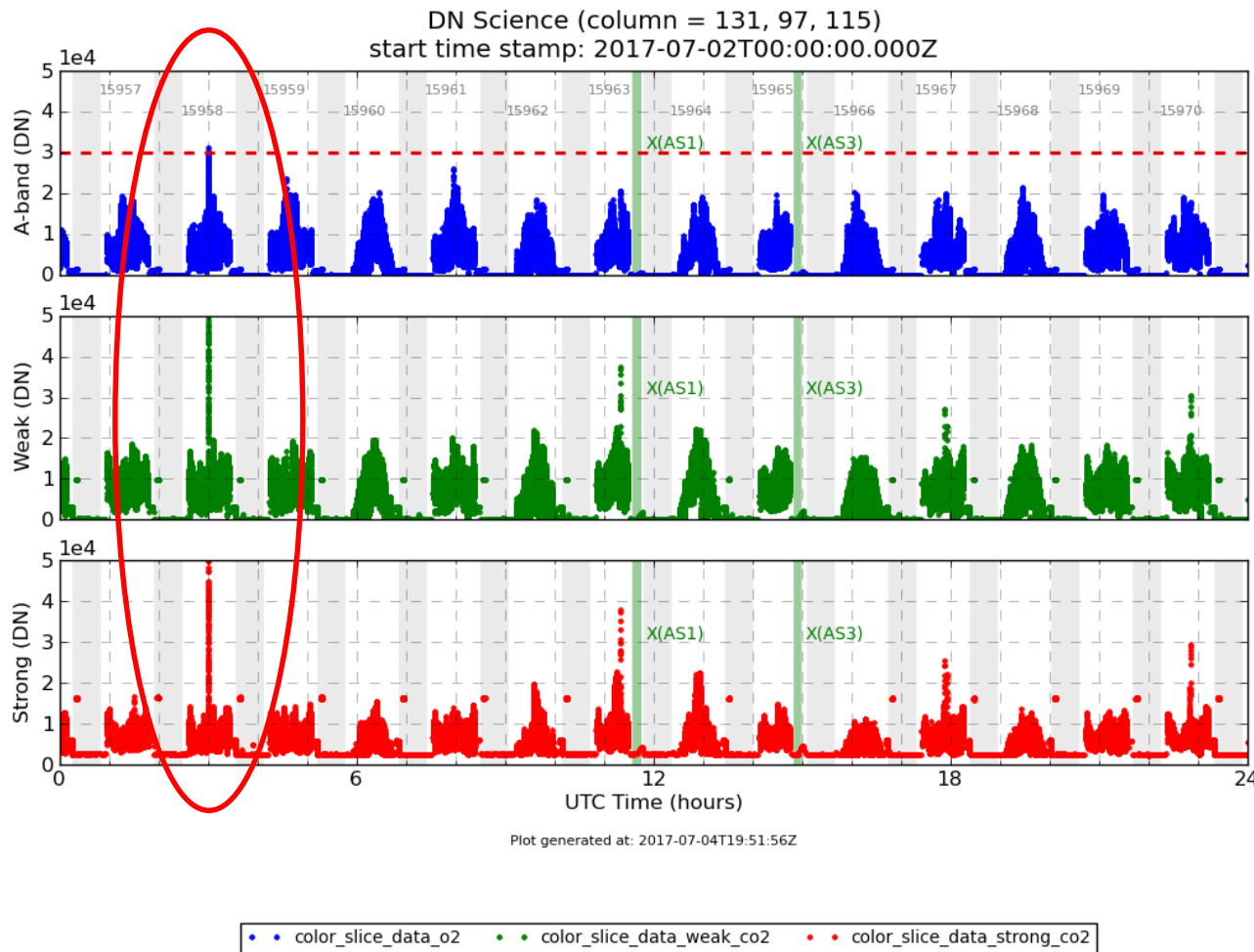
- An unexpectedly bright reflection off Lake Maracaibo in Venezuela saturated all 3 detectors, leading to concerns about instrument safety
- Changes to the glint pointing offset were considered, but then rejected since the incident posed no danger to the system, and any change would reduce signal levels at high latitudes



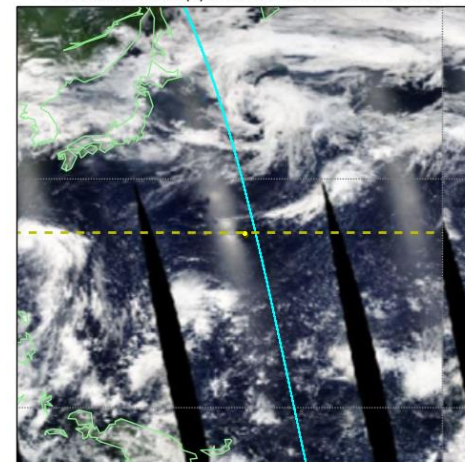
- Place: Lake Maracaibo, Venezuela
- Date and Time:
 - 7 August 2014
 - 18:11:00.666 UTC



Possible Saturation Event: July 2, 2017, Orbit 15958



Saturation event(s) for 2017-07-02. Orbit: 15958

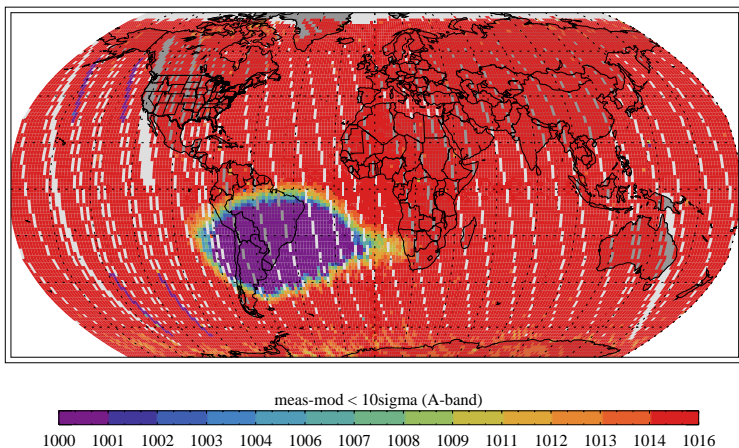


A bright ocean glint exposure southeast of Japan exceeded the saturation warning limits. These events are more common during the summer due to the sun's beta-angle.

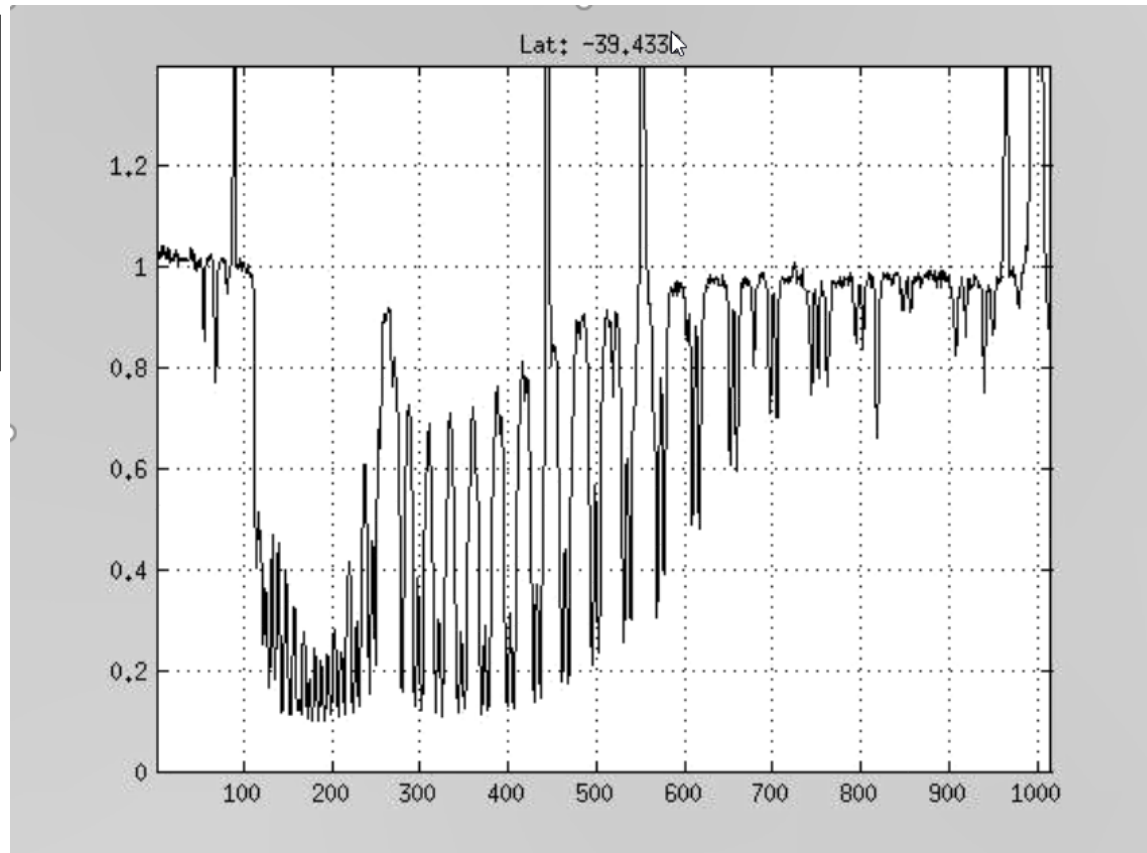


Calibration Challenges: Cosmic Rays

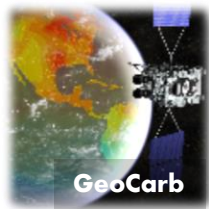
Cosmic rays a particular problem, especially on orbits that pass through the South Atlantic Anomaly (i.e. just about every orbit over South America)



- The largest effects are seen in the O₂ A-band.
- An algorithm to screen the specific colors affected by cosmic rays has been implemented.



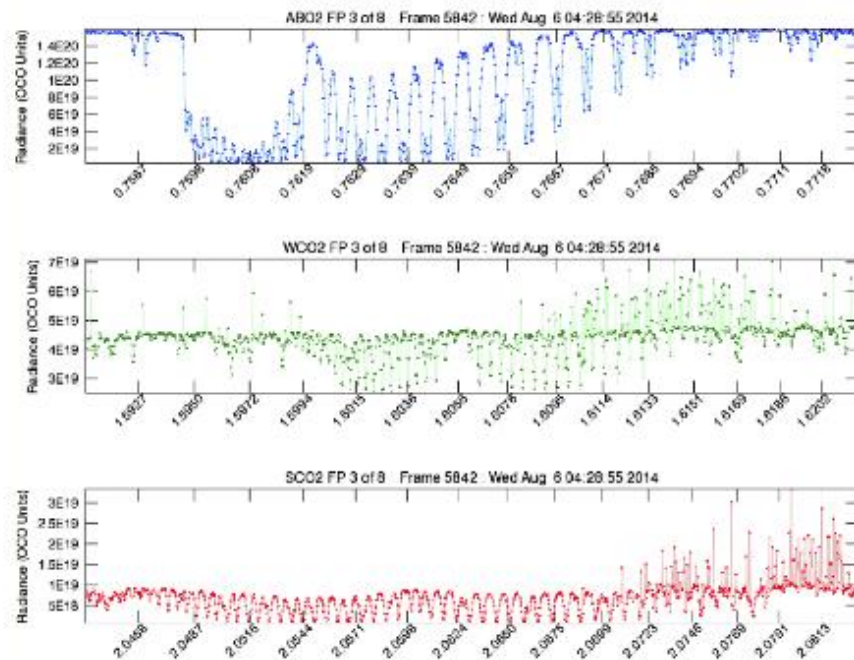
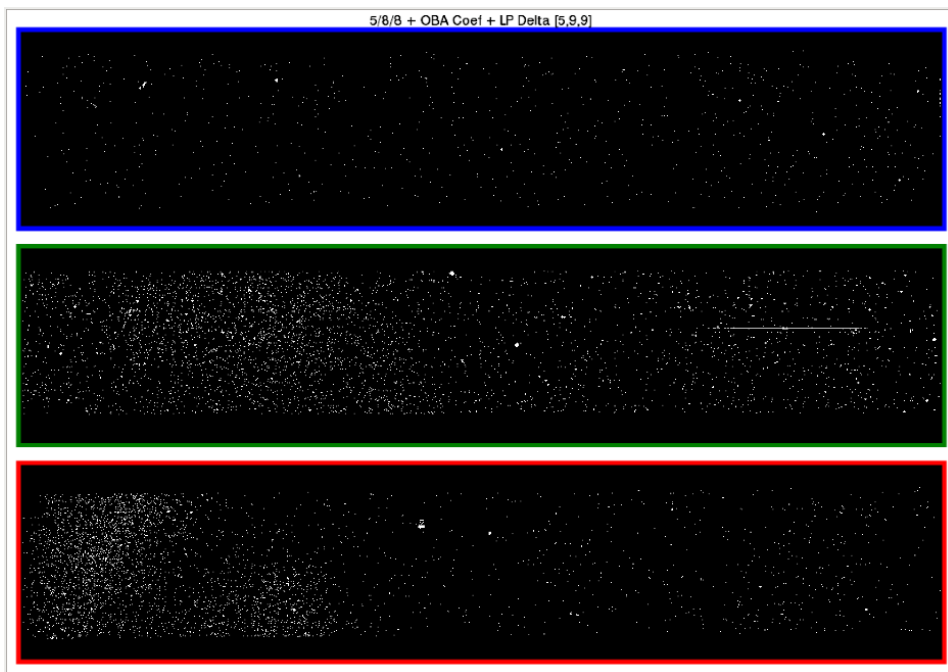
OCO-2 A-band spectra from the South Atlantic Anomaly



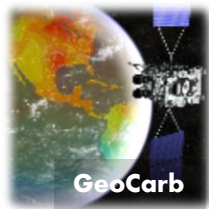
Bad Pixels

The number of bad pixels increased substantially between the pre-flight testing (April 2012) and launch (July 2014)

- Improved bad pixel maps were an early focus of Calibration team

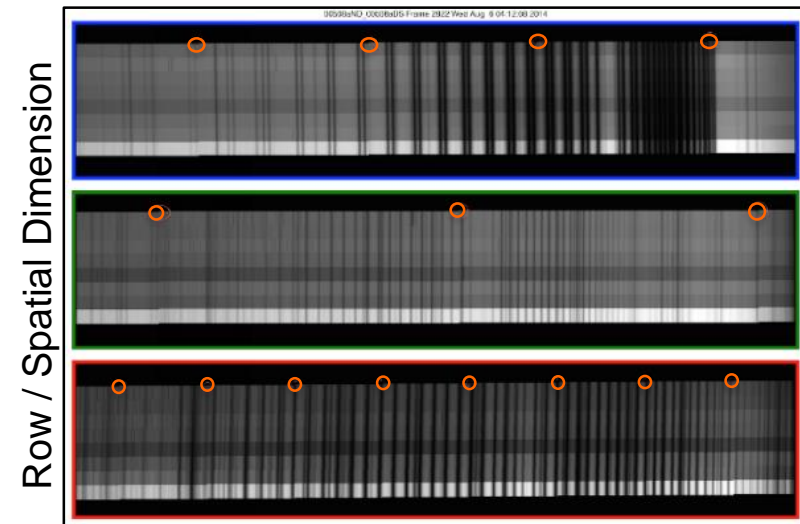


Bad pixels (left) are shown along with their associated bad samples (right) for the A-Band (top), Weak CO₂ (middle) and Strong CO₂ (bottom) channels

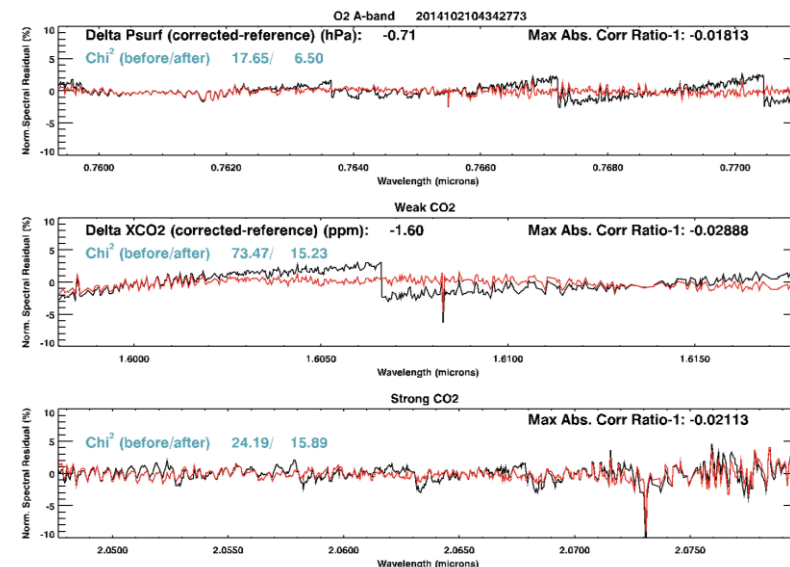
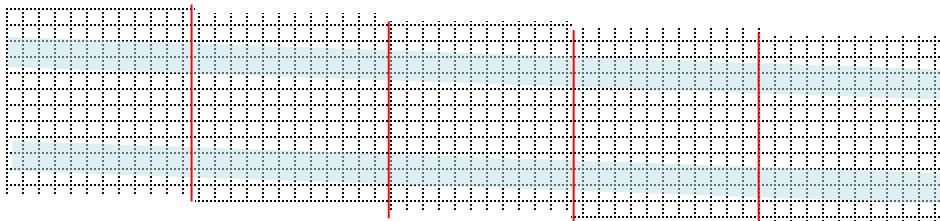


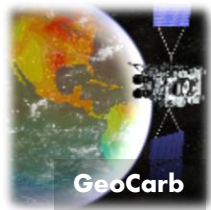
Radiance Discontinuities due to FPA Rotation (Clocking)

- The OCO-2 FPA's are rotated slightly with respect to the slit and grating
- With these *FPA Clocking Errors*, the FPA rows recording a given spatial footprint varies across the spectral range (columns)
- To record the same spatial footprint across an entire spectrum, the starting pixel of each spatial footprint can be adjusted from one column (wavelength) to another (by one pixel)



Christian Frankenberg & Fabiano Oyafuso



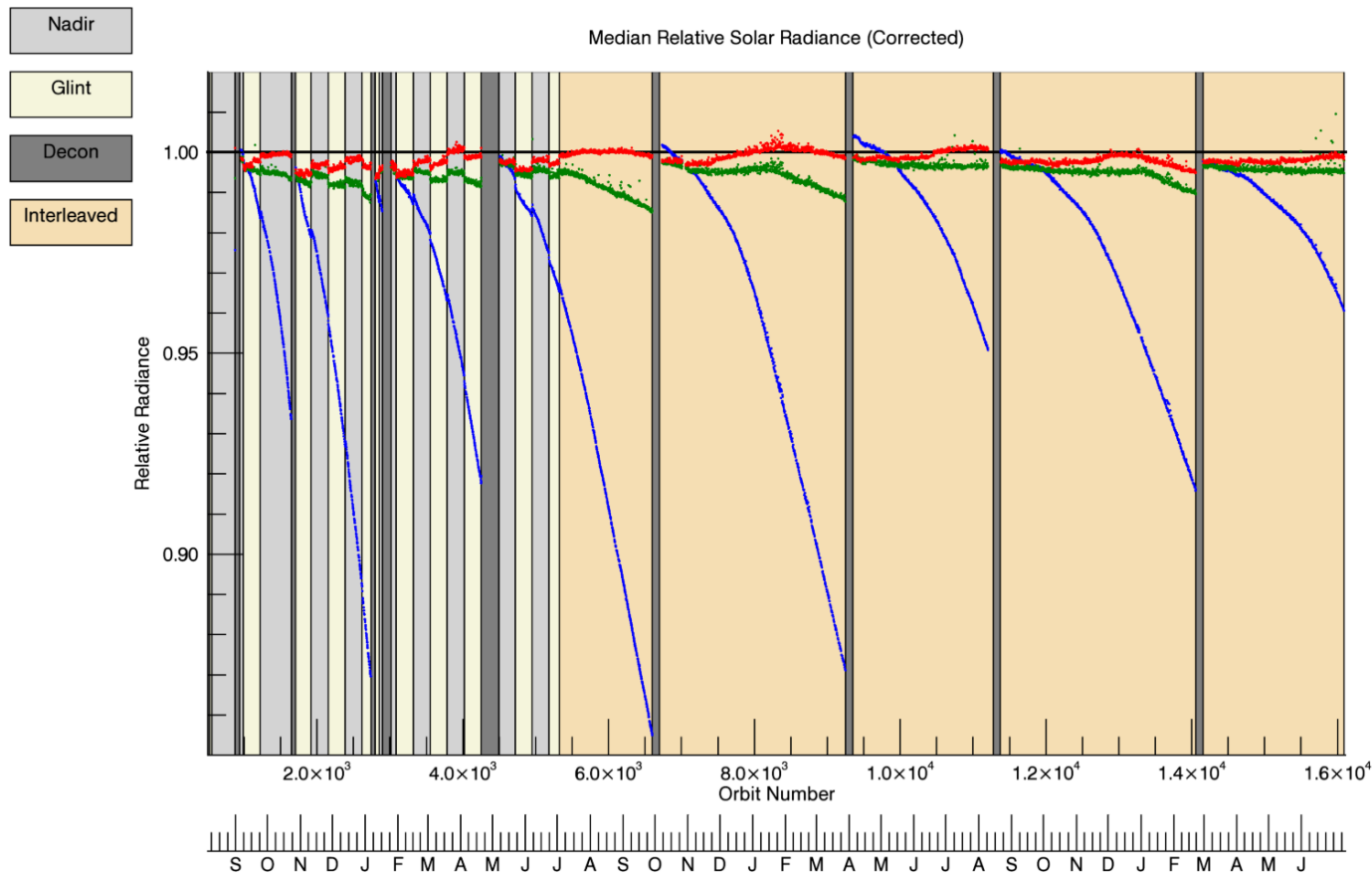


A-Band Channel Sensitivity Variations

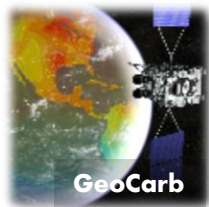
- The sensitivity of the OCO-2 ABO2 channel has varied over time, while the WCO2 and SCO2 show much less variability
- The ABO2 sensitivity degradation has two components
 - A “fast degradation” reversed by decontamination activities
 - This component has been attributed to temporary degradation of the anti-reflection coating on the A-band focal plane array detector (FPA) due to the accumulation of a thin (< 100 nm) layer of ice on the FPA
 - A monotonic “slow degradation”
 - Lunar and Vicarious Calibration measurements indicate that this change is due to degradation of the solar diffuser rather than a throughput loss in the instrument



OCO-2 O₂ A-band Sensitivity Degradation

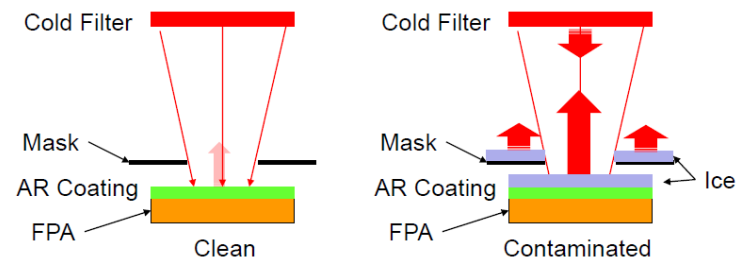


Observations of diffuse sunlight obtained on each orbit show systematic decreases in the throughput of the O₂ A-band channel (blue points) between decontamination cycles (grey bars). The weak and strong CO₂ channels (green and red points) show much less variation.

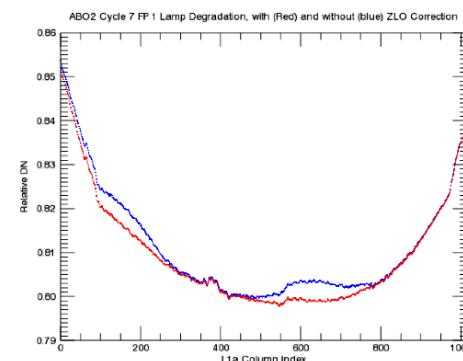
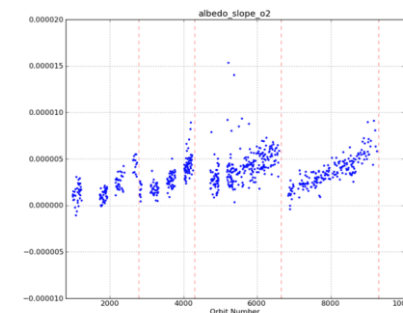


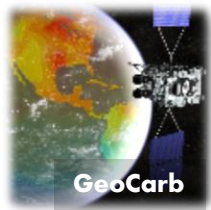
Correcting for the impact of ice accumulation on the FPAs

- The “fast degradation is associated with ice accumulation on the A-band (ABO2) focal plane array (FPA), that degrades the performance of the anti-reflection coating
- The ice contamination also introduces a zero level offset (ZLO), which in turn introduces artifacts in the SIF and aerosol retrievals
- Both the reduced signal and the zero level associated with ice accumulation and the ZLO produced by the scattered light are corrected in version 8 L1B radiances

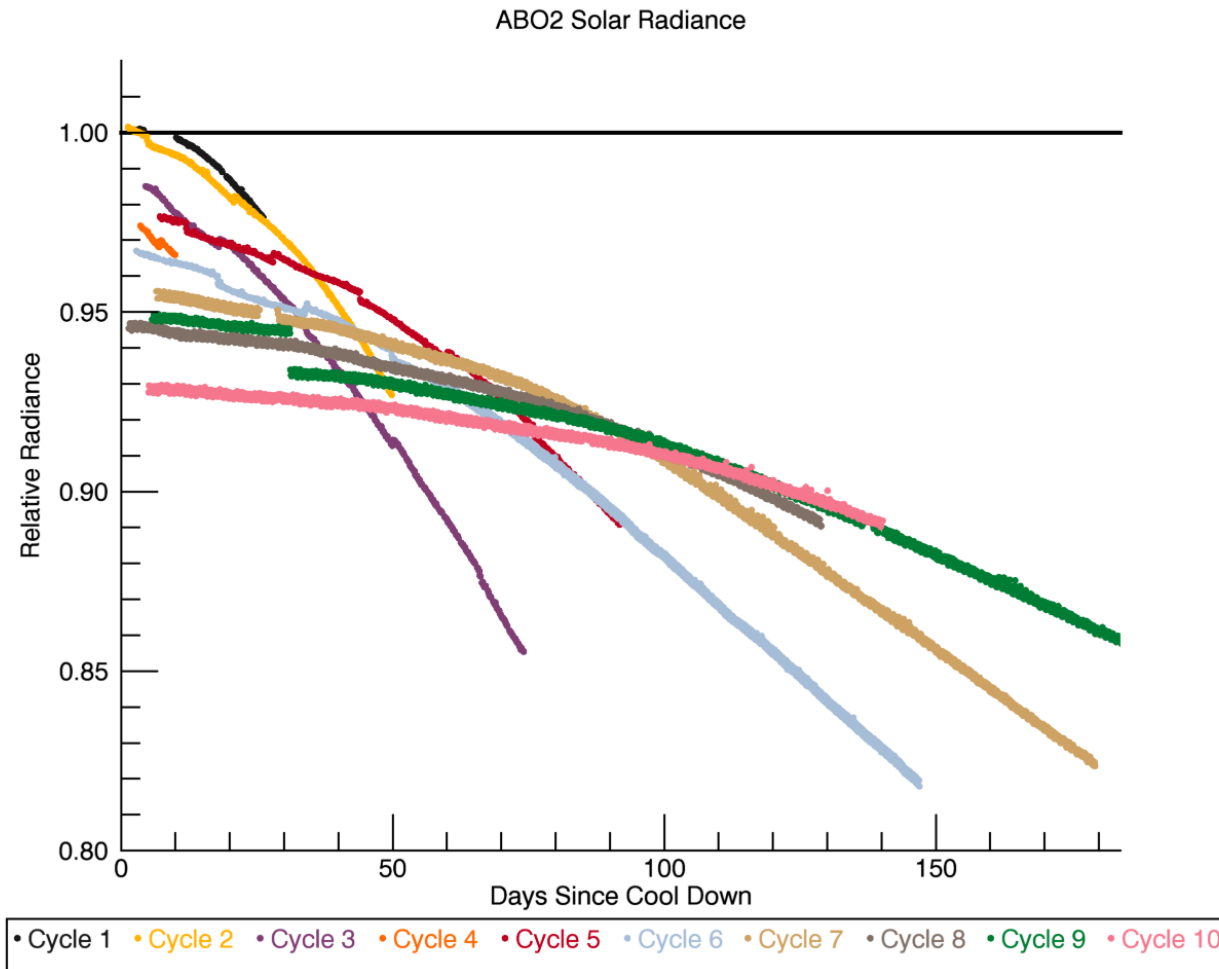


pre-v8 Apply EOF results: O2A Alb Slope

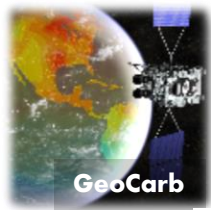




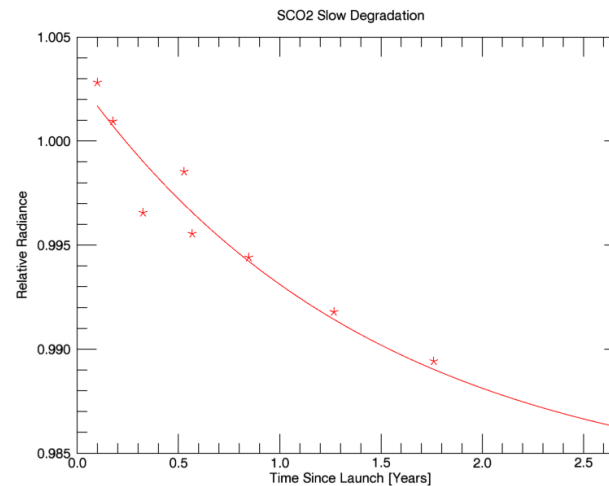
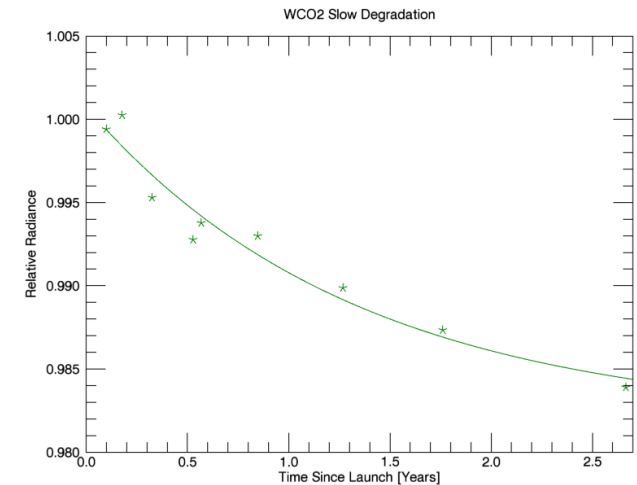
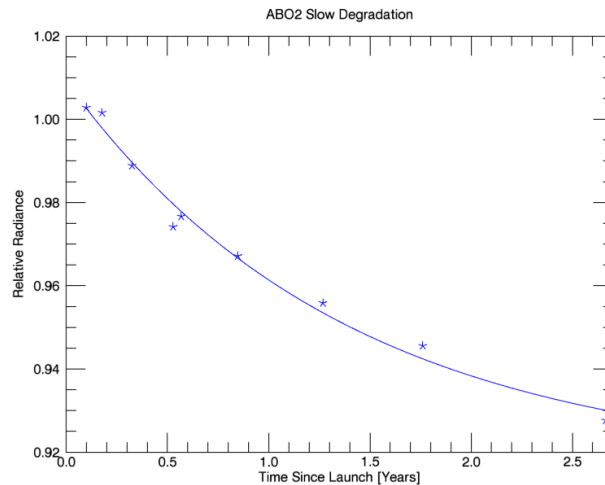
FPA Ice Accumulation Rate



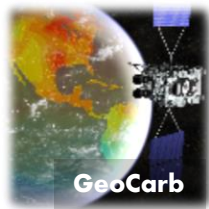
The ice accumulation rate on the ABO2 FPA continues to decrease with time.



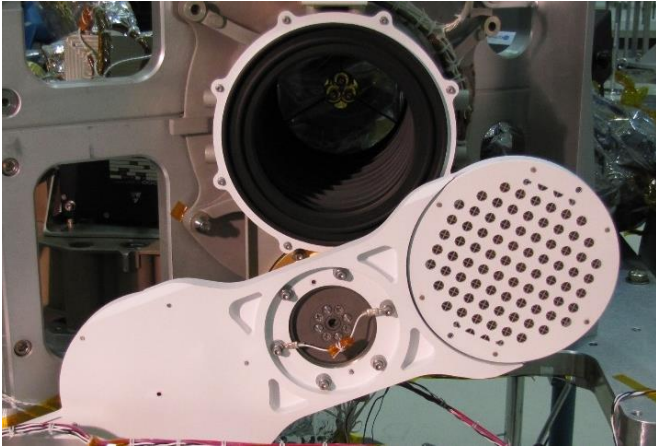
Slow Degradation of the Solar Diffuser



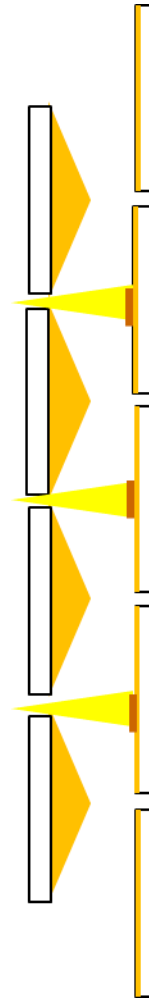
Monthly Lunar observations show that the “slow degradation” is primarily due to secular changes in the solar diffuser rather than then science optical path.



The Slow Degradation Mechanism



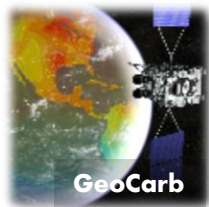
The solar diffuser consists of a pair of plates with a series of pin holes that are offset from each other, with a gold coated internal surface



Hypothesis;

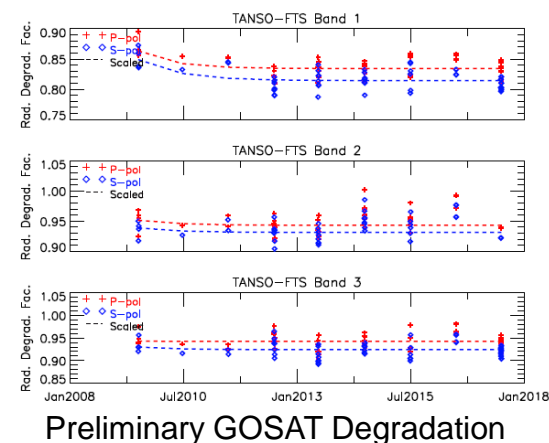
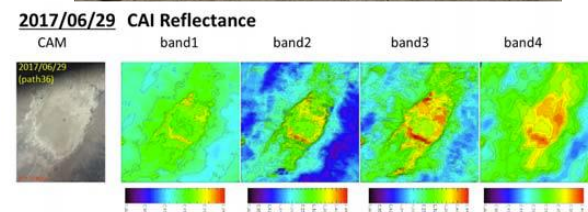
- As solar UV interacts with contaminants on the gold coated inter surface, it causes darkening.
- The most severe darkening is expected in the ABO2 Channel
- The rate of the darkening is uniform, but could not be predicted prior to launch.

Cartoon showing basic principle only



The 2017 Railroad Valley Campaign was a Success

- Team deployed in RRV on 25-30 June
 - Ground based data collected on 25 (“training day”), 26, 27, 29 and 30 June
 - No rain and cloud-free skies on 25-23 June
 - Slightly hazy on 6/26
 - Alpha Jet not available
- OCO-2 Target Observations
 - 2017-06-25 14:05:28 PDT (2017-06-25 21:05:28 UTC)
 - 2017-06-27 13:53:08 PDT (2017-06-27 20:53:08 UTC)
 - 2017-06-29 13:41:00 PDT (2017-06-29 20:41:00 UTC)
- GOSAT Target Observations
 - Path 36 (east: forward scattering) on 2017-06-26 and 2017-06-29 (“Golden Day”)
 - Path 37 (west, backscattering) on 2017-06-27 (Silver day) and 2017-06-30 29
- Followed by a 1-day Salton Sea Campaign





Summary

- The OCO-2 instrument was extensively characterized and calibrated prior to launch
- As always happens, the instrument you test on the ground is not the one that arrives in space
 - Significant increase in bad pixels in CO₂ bands
 - Sensitivity to non-uniformly illuminated footprints
- Occasionally, you miss things in ground testing
 - Performance reserve is a major contributor to mission success
- Characterizing and correcting for these issues on orbit has been a challenge, but has been enabled by a robust calibration program
- GeoCarb will face many of these challenges, as well as others associated with:
 - The 2.3 micron channel, which is not shared by OCO-2
 - Those specific to its geostationary vantage point